SWECLIM
SWEDISH REGIONAL CLIMATE MODELLING PROGRAMME

SMHI

No. 27, 1999

Reports Oceanography

10-year mean heat flux, RCA1 (22 km)

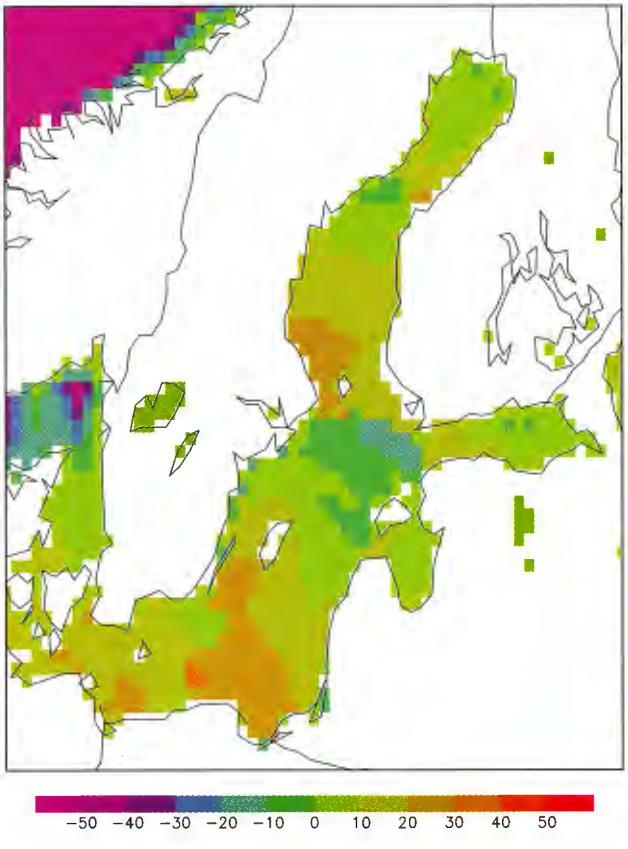

13-year mean heat flux, RCO1 (6nm)

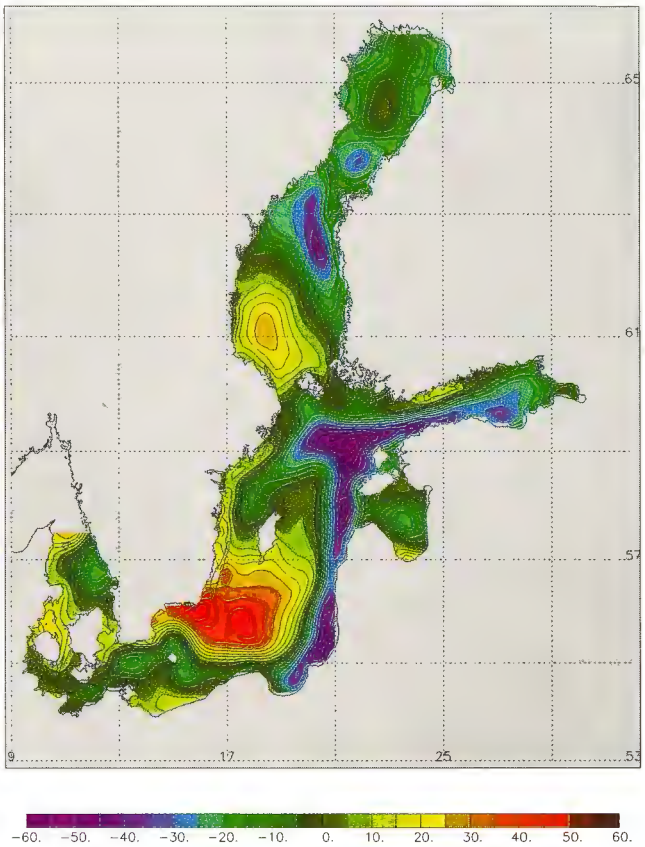

First results of multi-year simulations using a 3D Baltic Sea model

H.E. Markus Meier
Rossby Centre

Cover illustration: 13-year mean heat flux from RCO 1.0 hindcast run, $6\,nm$, for the period 1980-1993 (right panel) compared with 10-year mean heat flux from RCA1 control run, $22\,km$ (left panel). Positive values indicate fluxes (in $W\,m^{-2}$) into ice or ocean.

RO
No. 27, 1999

First results of multi-year simulations using a 3D Baltic Sea model

H.E. Markus Meier
Rossby Centre

Report Summary / Rapportsammanfattning

Issuing Agency/Utgivare	Report number/Publikation
Swedish Meteorological and Hydrological Institute S-601 76 NORRKÖPING Sweden	RO No. 27
	Report date/Utgivningsdatum October 1999

Author (s)/Författare
H. E. Markus Meier

Title (and Subtitle/Titel

First results of multi-year simulations using a 3D Baltic Sea model

Abstract/Sammandrag

Results of 13-year hindcast simulations for the period 1980-1993 are presented using a 6 nm version of RCO (the Rossby Centre Ocean model). The coupled ice-ocean model for the Baltic Sea with open boundary in northern Kattegat is forced with realistic atmospheric forcing and river runoff. The results are compared to monitoring temperature and salinity profile data, mean sea surface height, ice extent and ice thickness data. The model performance is regarded as good. For example, erosion of the halocline in the Baltic proper could be avoided due to carefully chosen parameterizations. However, it is necessary to extend the model domain, to embed a bottom boundary layer model (or to increase horizontal resolution) and to include more ice classes.

Furthermore, a set of sensitivity and process oriented studies are performed to increase our understanding of the processes involved. Thereby, different mixing parameterizations, advection schemes and open boundary data are tested. Experiments with and without wind, present day and increased runoff, with and without ice or with and without ice dynamics are compared and analyzed. The results show that the mean wind-driven circulation affects mean SST's and SSH's. Mean Ekman transport is added to the thermohaline vertical circulation causing a 3-layer transport system into the Gulf of Finland for example. Mean surface heat flux patterns are affected by horizontal advection, up- and downwelling and ice cover. Without ice heat loss in ice covered areas is increased tremendously. Ice dynamics re-distribute mean ice thickness and concentration from south-western to north-eastern parts in the Gulf of Bothnia. Increased river runoff causes a decrease of surface layer salinity and halocline depth in Gotland Basin. In Bornholm Basin mainly lower layer salinity is affected indicating reduced salt water inflow through the Danish Straits.

Key words/sök-, nyckelord
Baltic Sea, modelling, coupled ice-ocean, regional climate, multi-year simulations

Supplementary notes/Tillägg	Number of pages/Antal sidor	Language/Språk
This work is a part of the SWECLIM programme.	48	English

ISSN and title/ISSN och titel

0283-1112 SMHI Reports Oceanography

Report available from/Rapporten kan köpas från:

SMHI
S-601 76 NORRKÖPING
Sweden

Contents

1 Introduction

The hydrography of the Baltic Sea is determined mainly by four factors (Mälkki and Tamsalu, 1985):

- atmosphere-ice-ocean interaction
- water exchange through the Danish Straits
- river discharge
- bottom topography.

The water exchange and river runoff determine the stratification of the water masses into a homogeneous upper layer and a stratified lower layer. Due to the stratification, the atmosphere influences mainly the homogeneous upper layer although also the lower layer is affected. For example the internal wave field is governing deep water mixing. During the summer, the upper layer is heated and a seasonal thermocline is established. During late autumn and winter, vertical convection erodes the thermal stratification, resulting in the characteristic two-layer structure of the Baltic Sea. The bottom topography separates the subhalocline water masses into separate basins, delimited by high sills.

The Swedish Regional Climate Modelling Programme, SWECLIM, aims to increase our knowledge of effects of climate change in Sweden and the other Nordic countries (SWECLIM, 1998). Hence, the oceanography modeling activities within SWECLIM aim to simulate and to understand long-term changes of Baltic hydrography. The influence of the listed factors are investigated utilizing different numerical models of the Baltic Sea. Among these activities simulations of the hindcast period from May 1980 until December 1993 have been performed using the Rossby Centre Ocean model, RCO (Meier et al., 1999). These multi-year experiments have been done with the intention to validate the coupled ice-ocean model with available observations of the present climate, i.e., sea level, temperature, salinity, maximum ice extent and ice thickness data. Although the period of more than 13 years is not long enough to determine the Baltic Sea mean state, the model performance with respect to interannual variability can be tested. For example, sea ice seasons with mild, normal and severe winters are included in the test period as well as one major salt water inflow in January 1993 at the end of the hindcast period. The 16 year stagnation period between 1976 and 1992 serves as an excellent test for deep water parameterizations. Thereby, important requirements are to keep the stratification during the integration stable and to avoid artificial erosion of the halocline due to numerical shortcomings. Problems with discretization and parameterization schemes are often hidden in short simulations but will show up clearly during long-term integrations.

Nevertheless, the period 1980-1993 has been selected mainly due to the availability of homogeneous observational data sets for atmospheric variables and river runoff with sufficient quality to force a 3D Baltic Sea model. In addition, for model initialization and model validation a lot of measurements can be used whereas former periods are

characterized by less available data.

Furthermore, a set of sensitivity and process oriented studies have been performed. Thereby, different mixing and surface flux parameterizations, advection schemes and open boundary data have been tested. Experiments with reduced mean wind speed, completely omitted wind, increased river runoff, with ice dynamics and thermodynamics and with thermodynamics only have been performed and analyzed. The sensitivity studies aim to increase our understanding of the processes involved. Especially, the interest is focused on the mean circulation and on vertical and horizontal heat transports in the Baltic Sea and its long-term changes.

It is worth to stress that for the first time results from multi-year simulations (more than 10 years) using a 3D Baltic Sea model are presented and compared with observations. So far, long-term studies of the Baltic Sea were restricted to process oriented, horizontally integrated models (e.g., Stigebrandt, 1983; Omstedt and Nyberg, 1996; Omstedt, Meuller and Nyberg, 1997; Omstedt and Axell, 1998). Due to the computational burden of resolving the complicated bottom topography of the Baltic Sea 3D models have been used only for shorter integrations (e.g., Kielmann, 1978; Lehmann, 1995; Meier, 1996). The development of a coupled ice-ocean model based on massively parallel coding for use on super computers like a CRAY-T3E as described by Meier et al. (1999) allows now multi-year simulations within SWECLIM. Here, first results are presented.

The report is organized as follows: In the second section a short summary of changes for the used model version is given. For further information about the model configuration the reader is referred to Meier et al. (1999). Results of the validation are discussed in the third section. The mean state of simulated Baltic Sea variables and mean sea surface fluxes are presented in the fourth and fifth section, respectively. Results of selected sensitivity and process oriented studies are shown in the sixth section. The report ends with a summary.

2 Description of the model version

2.1 Resolution

For the multi-year simulations RCO version 1.0 as described by Meier et al. (1999) has been used with a horizontal resolution of 6 nautical miles and 41 vertical levels with layer thicknesses between 3 and 12 m. Due to the computational burden the coarser horizontal resolution is necessary for the moment to perform many test runs of the long period.

2.2 Deep water mixing

The Baltic Sea is a stratified estuary with a halocline preventing surface generated wind mixing to influence deeper layers on seasonal time scale. However, for climate studies deep water mixing needs to be taken into account (Stigebrandt, 1987; Axell, 1998). The $k-\epsilon$ model is extended to include a parameterization for breaking internal waves:

$$\nu = \nu_t + \sigma_t \min\left(\frac{\alpha}{N}, \nu_{0,max}\right) . \tag{1}$$

Here, ν_t denotes turbulent viscosity, σ_t turbulent Prandtl number, N Brunt-Väisälä frequency, α and $\nu_{0,max}$ constants. Different values for the mixing parameter α have been tested in the range $\alpha = 0.5 - 2 \cdot 10^{-3}\, cm^2\, s^{-2}$. Correspondingly, the maximum background mixing has been chosen to $\nu_{0,max} = 0.5 - 2\, cm^2\, s^{-1}$. The turbulent Prandtl number is calculated from an empirical formula which depends on the Richardson number (Blanke and Delecluse, 1993). This and the $k-\epsilon$ model is described by Meier et al. (1999) and Meier (1999).

2.3 Forcing and initial data

The data sets as described by Meier et al. (1999) have been used as forcing (SMHI's atmospherical and hydrological data bases). Sea level data from the Swedish tide gauge Ringhals (Varberg) have been prescribed at the open boundaries of the model domain and in case of inflow temperature and salinity is relaxed towards climatological profile data from Kattegat. From observed temperature and salinity profiles initial conditions have been generated for May 26, 1980. The initialization and spin-up procedure is the same as for the shorter validation period 1992/93 and described by Meier et al. (1999) in detail.

2.4 Sea ice model

As in Meier et al. (1999) a thermodynamic-dynamic sea ice model with 2 levels (open water and level ice) has been used. There is no distinction between deformed and undeformed ice yet. More sophisticated models as described by Haapala and Leppäranta (1996) or Haapala (1999) take different ice classes into account. In Meier et al. (1999)

only a simple parameterization for ridged ice to reduce ice growth for ice thicknesses above a certain threshold has been utilitized. It turned out that this results in too small ice thicknesses in some years. Hence, no parameterization for ridged ice is used in this report. To avoid unrealistic ice growth minimum bottom heat fluxes between ocean and ice have been optimized to simulate observed ice thicknesses during the whole 13-year period (cf. Eq.110 with $\Delta u_{min} = 0.1\,cm\,s^{-1}$ and $\Delta T_{min} = 0.6\,°C$ by Meier et al., 1999).

3 Model-data comparison

3.1 Temperature

The results of the 13 year long simulation have been compared to monitoring profile data from the Swedish Ocean Archive SHARK (Svenskt HavsARKiv, SMHI). The analysis was focused on Kattegat (Anholt East, AE), Arkona Basin (Arkona Deep, BY2), Bornholm Basin (Bornholm Deep, BY5), Eastern Gotland Basin (Gotland Deep, BY15) and Northwestern Gotland Basin (Landsort Deep, BY31). The locations of the monitoring stations are depicted in Figure 5 by Meier et al. (1999).

Figure 1 shows observed (a) and simulated (b) isotherm depths from May 1980 until July 1993 at Gotland Deep. For this time period 102 profiles with sufficient quality are available. The model profiles have been extracted at the same dates as the data to avoid the comparison between highly resolved model results and undersampled observations. The seasonal cycle of the thermocline in Gotland Basin and the other sub-basins is simulated in good agreement compared to the data. There is slight underestimation of mixed layer depth in some years indicating inaccuracy of the atmospheric forcing data. No systematic trends have been observed indicating shortcomings of the turbulence model. The initial profile for Gotland Basin taken from the observations is obviously too warm causing the difference between simulated and observed deep water temperature. The decrease of temperature follows the decrease of salinity in the deep water (see next subsection).

Another example is shown in Figure 1c and 1d. In the shallower ($100\,m$ deep) Bornholm Basin the seasonal wind mixing influences the whole upper layer of the water column above the halocline where the salinity is almost constant. For Bornholm Deep 193 observed profiles have been used. The agreement is as good as for the Gotland Deep. In some years the mixed layer depths in summer are underestimated.

3.2 Salinity

Figure 2 shows observed and simulated isohaline depths at Gotland Deep. During the 16 year long stagnation period between 1976 and 1992 the salinity in the deeper layer of the Baltic Sea decreases remarkable. For comparison 3 different simulations

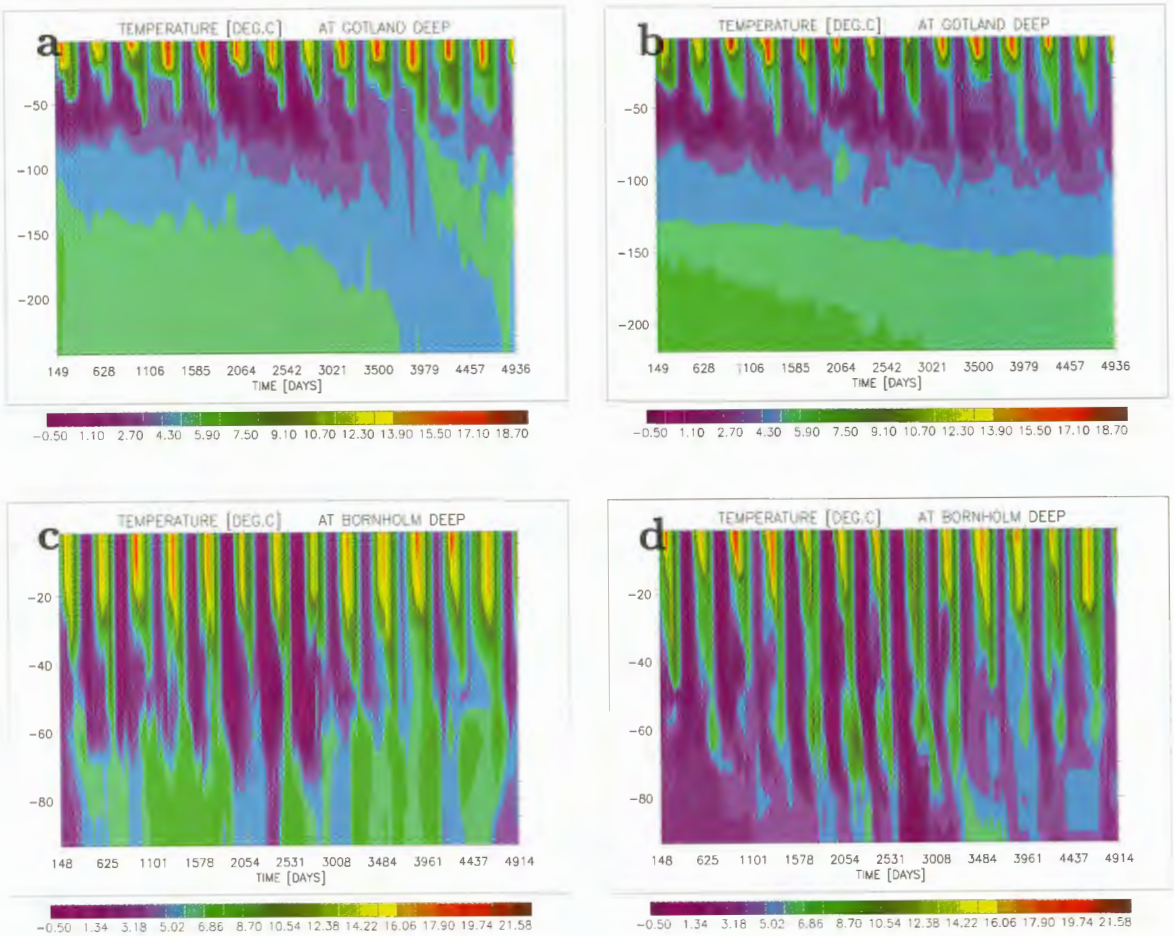

Figure 1: *Observed (a) and simulated (b) isotherm depths (in °C) from May 1980 until July 1993 at Gotland Deep and observed (c) and simulated (d) isotherm depths from May 1980 until June 1993 at Bornholm Deep. The counting of days start at January 1, 1980.*

are shown: without deep water mixing (Fig.2b) and with deep water mixing parameterization and two different mixing constants (Fig.2c: $\alpha = 0.5 \cdot 10^{-3}\, cm^2\, s^{-2}$, Fig.2d: $\alpha = 1.0 \cdot 10^{-3}\, cm^2\, s^{-2}$). The diffusion across the halocline in case without deep water mixing (b) is too small compared with the observations (a). Hence, it is important to add a parameterization for deep water mixing. (c) and (d) show simulation results with deep water mixing included using two different mixing coefficients. The optimized value for the constant α at Gotland Deep is somewhere between 0.5 and $1.0 \cdot 10^{-3}\, cm^2\, s^{-2}$. This finding is remarkable because it agrees well with results from the North Atlantic. Oschlies and Garçon (1999) used an optimized value of $\alpha = 0.57 \cdot 10^{-3}\, cm^2\, s^{-2}$ within an eddy-permitting coupled physical-biological model of the North Atlantic. The value has been calculated from diffusivities of a tracer-release experiment described by Ledwell at al. (1993). On the other hand, Axell (1998) estimated from profile data of the Baltic Sea from the period 1964 until 1997 using a budget method an annual mean value of α for Gotland Deep of $1.5 \cdot 10^{-3}\, cm^2\, s^{-2}$ at two different depths. This is very close to the value obtained by Stigebrandt (1987) in his horizontally integrated model for the Baltic proper. In that model, Stigebrandt tuned α until the observed and computed

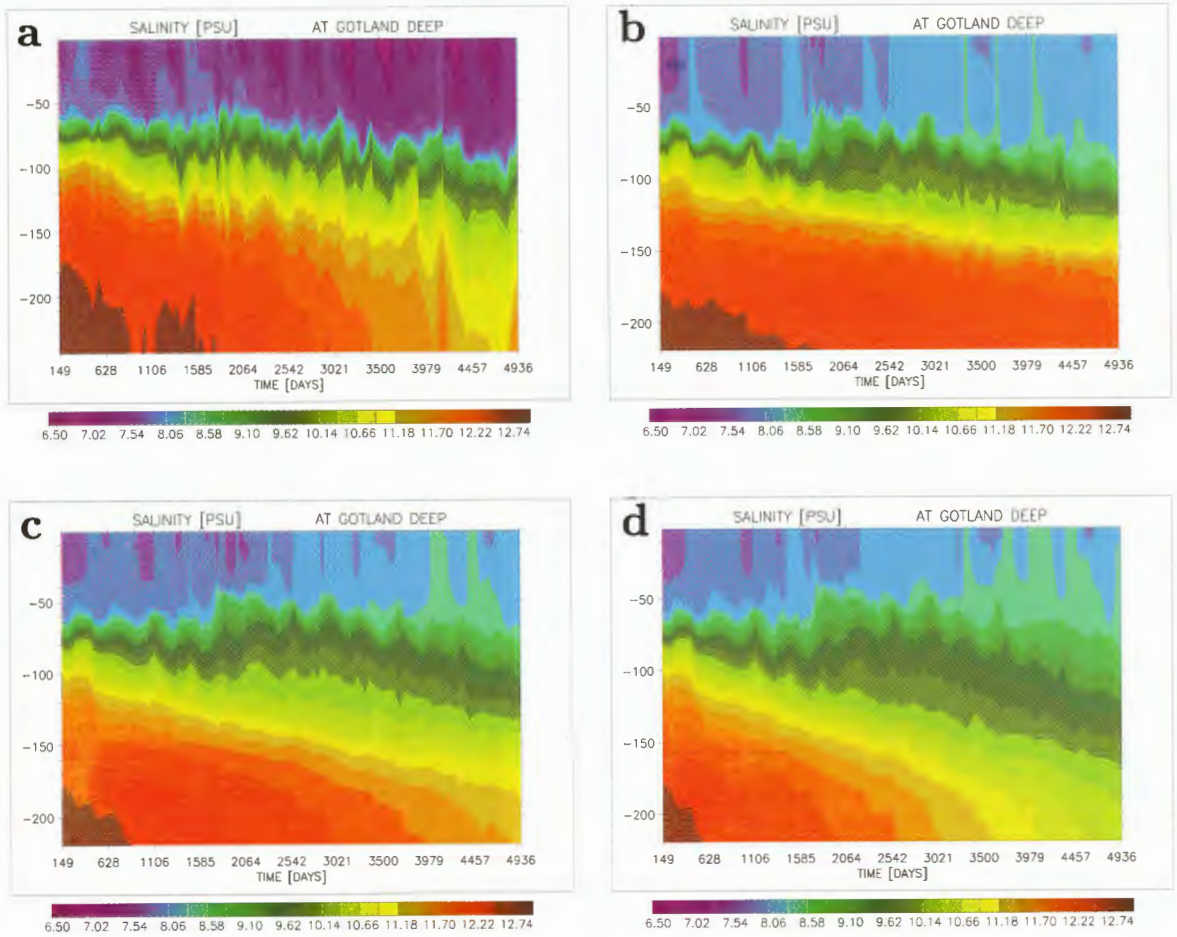

Figure 2: *Observed (a) and simulated (b, c, d) isohaline depths (in PSU) from May 1980 until July 1993 at Gotland Deep. In (b) results without parameterization for deep water mixing are depicted whereas in (c) and (d) an inversely proportional Brunt-Väisälä dependent background mixing is added with* $\alpha = 0.5 \cdot 10^{-3}\, cm^2\, s^{-2}$ *(c) and* $\alpha = 1.0 \cdot 10^{-3}\, cm^2\, s^{-2}$ *(d). The counting of days start at January 1, 1980.*

evolutions of the stratification agreed ($\alpha = 2 \cdot 10^{-3}\, cm^2\, s^{-2}$). Further, Axell (1998) has shown that there was a seasonal variation of the vertical diffusion well below the pycnocline and that diffusion was higher at Landsort Deep (closer to the coast) than at Gotland Deep. Obviously, α depends on local fluxes from energy sources, such as wind-driven inertial currents, Kelvin waves and other coastal trapped waves. Further investigations are necessary to elucidate this problem and to find better appropriate parameterizations for deep water mixing.

The agreement between model results and observations as shown in Figure 2 is good but with increasing deep water mixing the isohalines in the range from 9 to 10 PSU tend to diverge during the integration which is not observed. Obviously the parameterization for deep water mixing has undesired side-effects and needs to be improved.

Figure 3 shows observed (a) and simulated (b) isohaline depths at Bornholm Deep and observed (c) and simulated (d) isohaline depths at Anholt East. In (b) and

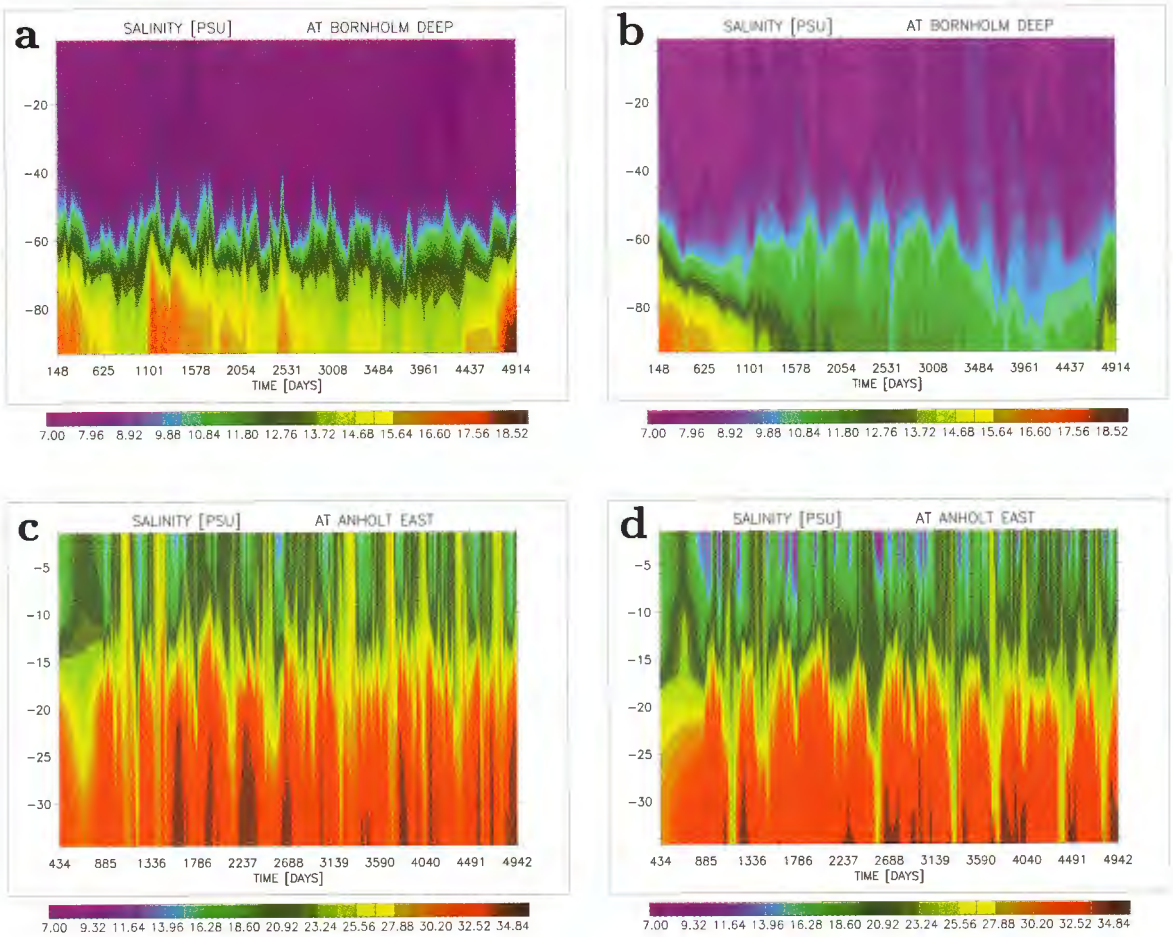

Figure 3: *Observed (a) and simulated (b) isohaline depths (in PSU) from May 1980 until June 1993 at Bornholm Deep and observed (c) and simulated (d) isohaline depths from March 1981 until July 1993 at Anholt East. The counting of days start at January 1, 1980.*

(d) model results are depicted considering the parameterization of deep water mixing ($\alpha = 0.5 \cdot 10^{-3}\, cm^2\, s^{-2}$), i.e., the corresponding results for Gotland Deep are shown in Fig.2c. As explicit deep water mixing alters the results for the western Baltic Sea only slightly, the too low salinity in the Bornholm Basin deep water must have other reasons. The initial decrease in salinity during the first 1000 days is simulated realistically. As shown in Section 6.2 the reason for too less salinity in the deep layer is caused by underestimation of inflowed salt water from Kattegat into Bornholm Basin. A detailed analysis showed that most of the salt water events occurred when they are observed but maximum salinities were too low. For example the major Baltic inflow event in January/February 1993 is simulated with maximum bottom water salinities of less than $15\,PSU$ instead of more than $18\,PSU$ as observed. It is important to note that still a salt water inflow occurred after almost 13 years of integration. The model deficits in case of overflow of the present coarse resolution version RCO 1.0 are discussed in Section 6.2. Starting the model with initial conditions from May 1992 much better results for the inflow event are obtained (Meier and Krauß, 1994; Meier, 1996; Meier et al., 1999).

For the monitoring station Anholt East in Kattegat 233 profiles of sufficient quality are available. Figure 3c and 3d show observed and simulated isohaline depths, respectively. In Kattegat the depth of the halocline is simulated correctly and the salinity of the deep water is close to 33.5 PSU, the climatological value for the period 1980 until 1993. The agreement between data and model results is very satisfactory. However, during single events surface salinity tends to be too low. This happens in distinct outflow situations and in situations of high wind speeds when wind generated turbulence causes mixing across the halocline. Obviously, the turbulence model generates too less mixing in case of a highly stratified water column.

3.3 Sea level

Figure 4 shows simulated 12-year mean sea surface height. The mean sea level increases from Kattegat to the Gulf of Bothnia and to the Gulf of Finland with about 25 to 35 cm. The slope is caused by freshwater supply of rivers located mainly in the northern and eastern parts of the Baltic Sea. In addition, the mean wind speed from South-West direction contributes to the slope in sea surface height (see Section 6.3). Also shown in Figure 4 are values of the mean sea level of selected tide gauge positions in comparison to the geoid solution of Ekman and Mäkinen (1996). They designed a consistent height system for comparisons between geodesy and oceanography for the Baltic Sea area. Ekman and Mäkinen (1996) computed mean sea surface topography geodetically in this height system at 42 reliable long-term sea level stations, connected by high-precision levelings, along the coasts of the Baltic Sea, the Kattegat, the Skagerrak and the adjacent part of the North Sea. The agreement between mean sea surface height in RCO and the geodetic result is very good. Differences occur only in the Kattegat and Baltic entrance area and in the Gulf of Finland. As RCO is used with the coarse horizontal resolution of 6 nautical miles the topography of the Danish Straits is not well represented in the model and had to be changed artificially. Especially, volume transports through the Sound cannot be correct. Hence, observed and simulated sea surface heights are different in the Danish Strait region. The reason for higher mean sea level in the Gulf of Finland might be an overestimation of mean wind speed in the atmospheric data set (see the discussion in Section 6.3).

3.4 Sea ice

Prognostic variables of the ice model are ice velocities, ice thickness, ice concentration, snow thickness, heat content of brine, surface temperature, temperature of snow layer and temperature of ice layers. As observations for most of these variables are missing, especially for long-term integrations, the validation is focused on ice extent and ice thickness. Statistical data can be found in "Climatological Ice Atlas for the Baltic Sea, Kattegat, Skagerrak and Lake Vänern (1963-1979)" published by the Swedish Meteorological and Hydrological Institute and the Finnish Institute of Marine Research (SMHI and FIMR, 1982). However, colder winters occurred during the period 1963-1979 than

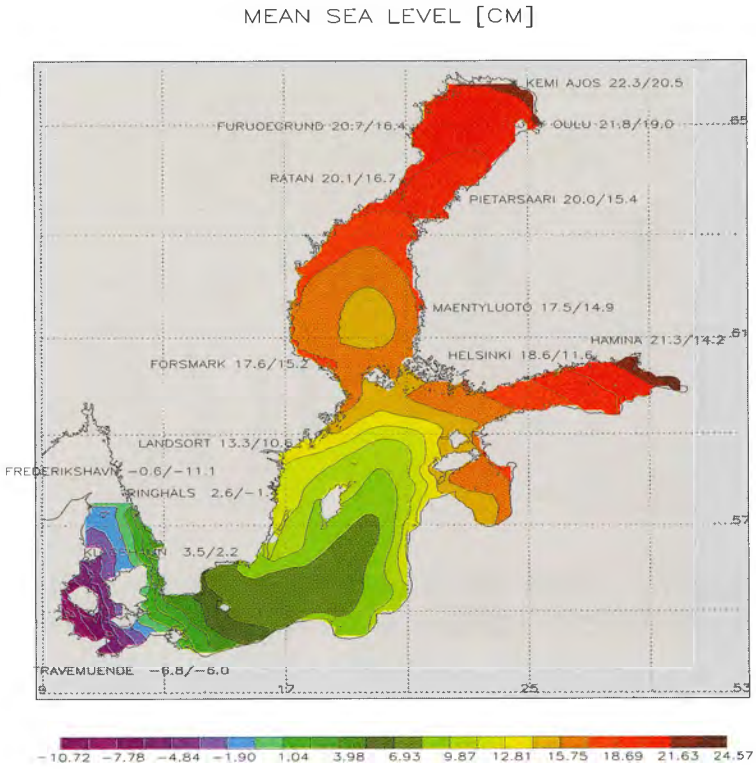

Figure 4: *Mean sea surface height (in cm) for the period May 27, 1980 until May 26, 1992. The numbers at selected tide gauge positions indicate model results (left) and geoid solutions of Ekman and Mäkinen (1996) (right).*

during the simulation period 1980-1993.

3.4.1 Ice extent

Figure 5 show simulated total ice extent compared with the observed maximum ice extent. Ice extent is highly correlated with air temperature but represents also a sensitive measure of ice model performance. The model must cover the high variability of observed ice extent. Contrary, other variables like mean ice thickness of the Bothnian Bay have lower variability. Hence, the correspondence between model results and observations in Figure 5 is very encouraging. In some winters (mainly mild ones) maximum ice extent is somewhat overestimated. However, the overall agreement is good. That is also true for the date when the maximum ice extent occurred. There is only one exception (winter 1988/89) when the ice model predicted a higher ice extent much earlier than the observations.

3.4.2 Ice thickness at Kemi

Compared to measurements from single ice seasons (Seinä and Peltola (1991) and Seinä et al. (1996)) at the coastal station Kemi it seems that the ice model underestimates ice thicknesses in mild winters and overestimates ice thicknesses in severe winters (Fig.6).

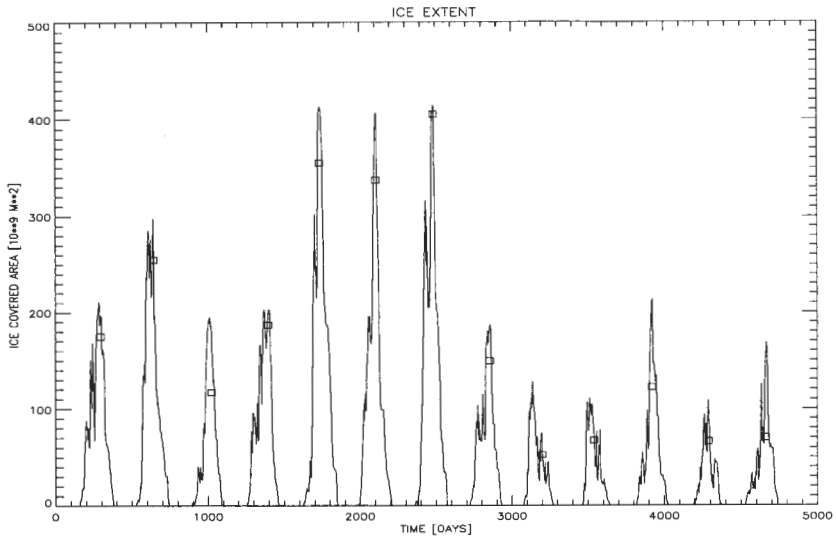

Figure 5: *Simulated ice covered area (in $10^9\,m^2$) for the period May 1980 until July 1993. Squares denote observed maximum ice extent (adopted from Omstedt and Nyberg, 1996).*

However, the detailed comparison with ice maps of the ice season 1992/93 for the whole ice covered area (see Meier et al., 1999) suggests that the overall ice thicknesses are simulated correct. A more systematic analysis comparing ice thickness distributions for different sub-basins is necessary to elucidate this point further. Improved horizontal ice thickness distributions are expected when ridged ice will be included. According to Bertil Håkansson (pers.comm.) the lack of snowice formation in the model might explain underestimation of ice thicknesses.

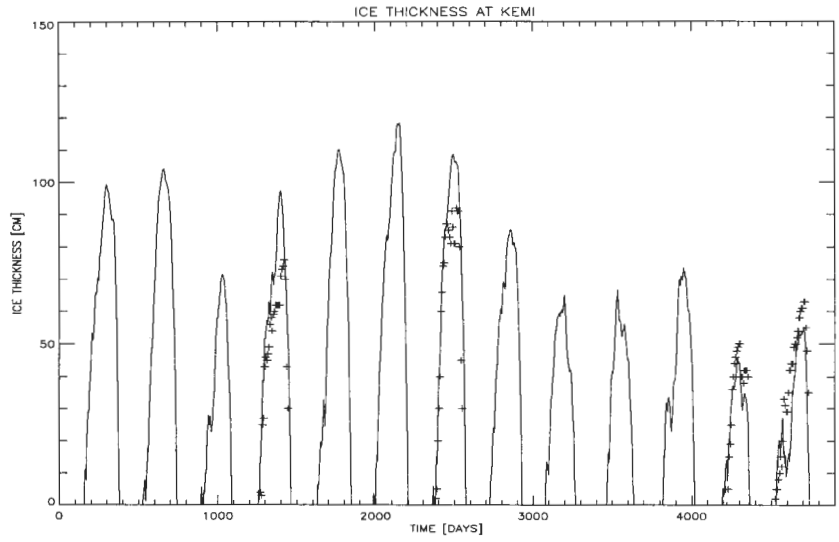

Figure 6: *Simulated ice thickness (in cm) for the period May 1980 until July 1993 at the monitoring station Kemi (Bothnian Bay). Plus signs denote observations from Seinä and Peltola (1991) and Seinä et al. (1996).*

3.4.3 Air temperature at Kemi

Maximum ice extent and air temperature in winter are highly correlated (see e.g., Omstedt and Chen, 1999). In Figure 7 air temperatures at the monitoring station Kemi in the Bothnian Bay for 3 selected years are depicted. The ice season 1983/84 is classified

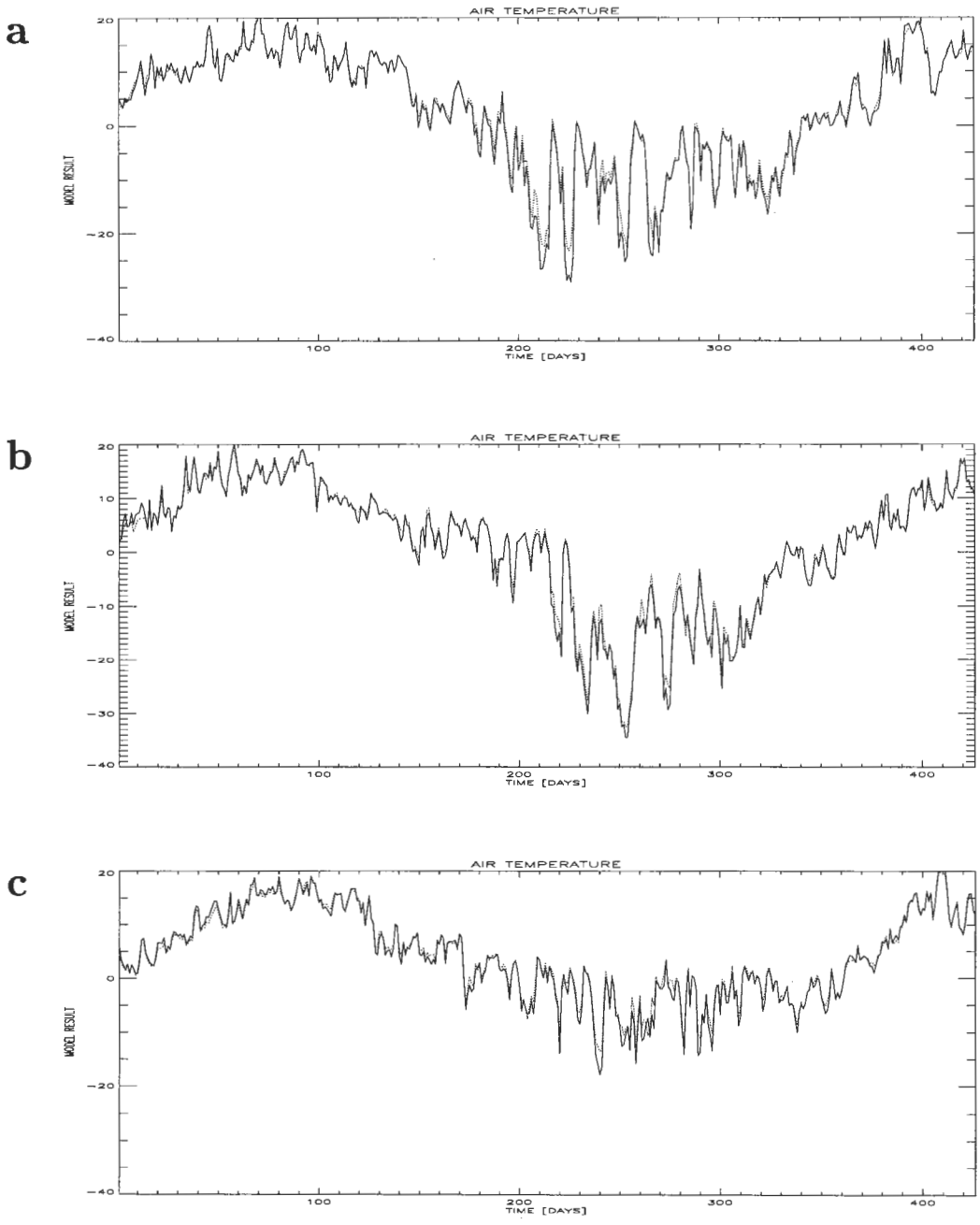

Figure 7: *Air temperature (in °C) for the periods 1983/84 (a), 1986/1987 (b), 1991/1992 (c) at the monitoring station Kemi. The time series start in May and end in June of the following year. The figure shows data from the Ice Data Bank (solid) and from the SMHI database (dashed).*

as normal, 1986/1987 as severe and 1991/1992 as mild winter (Haapala et al., 1996).

Comparing Fig.7 and Fig.5 the high correlation between both variables is obvious. The solid curves in Fig.7 denote observations from the Ice Data Bank (Haapala et al., 1996) and the dashed curves are extracted time records from the atmospheric forcing fields for RCO. These data are observations from the SMHI database which are interpolated first on a $1^o \times 1^o$ horizontal grid (Lars Meuller, pers.comm.) and second on the RCO model grid (Meier et al., 1999). To test how much the interpolation changes the original observations the two curves have been plotted together. The deviations are visible but quite small.

Shortcomings of the RCO atmospheric forcing are expected because most of the observations in the SMHI database are related to land stations. Thus, a cold bias of air temperature in winter over sea of the order of $2 - 3\,°C$ is very likely. This is approximately the 10-year mean winter (December/January/February) land-sea difference in $2\,m$ air temperature over the Bothnian Bay calculated from the RCA1 control run using the $22\,km$ horizontal resolution (Jouni Räisänen, pers.comm.). However, sensitivity experiments for the ice season 1992/93 have shown that this difference is too small to affect ice extent and ice thickness seriously.

3.4.4 Mean seasonal cycle of ice extent

Figure 8 shows observed and simulated mean time evolution of relative ice cover and standard deviations. The simulated period covers 13 ice seasons between 1980/81 and 1992/93. The observations were taken from "Climatological Ice Atlas for the Baltic Sea, Kattegat, Skagerrak and Lake Vänern (1963-1979)" (SMHI and FIMR, 1982) for the 6th, 16th and 26th for each month except February 25th (Jouni Räisänen, pers.comm.). The first value is for the 6th of November and the last for 26th of May. Thus, the ice atlas data covers 16 ice seasons (1963/64-1978/79).

Simulated mean time evolution and variability agree quite well with observations although the data originate from a different period. Obviously, simulated ice melt in spring occur earlier than in the observations. However, colder winters during 1963-1979 than during 1980-1993 might affect the mean melting dates. Both time periods are too short to determine a stable frequency distribution.

4 Mean ocean and ice variables

Several mean quantities like sea surface temperature, sea surface salinity, sea surface height, vertical integrated volume and heat transport, heat content, horizontal current velocity at different cross sections, ice thickness and ice concentration have been calculated. From these variables only mean sea surface height and mean time evolution of ice extent have been validated yet. A comparison with available climatological observations for temperature and salinity (Jansson et al., 1999) is still missing. However, one has to keep in mind that the averaging interval is only 13 years long which is too short to determine the mean state of the Baltic deep water. The renewal timescale of the

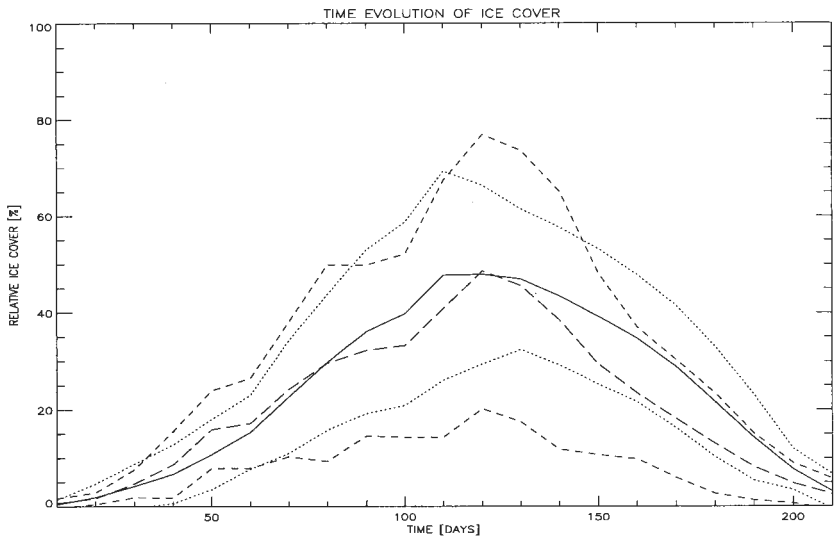

Figure 8: *Frequency distribution of Baltic Sea ice area. The long-dashed curve denotes the simulated mean time evolution of relative ice cover for the period 1980/81-1992/93. The two short-dashed curves shows the range of variability defined by added or subtracted standard deviations. Correspondingly, is the solid curve the observed mean time evolution of ice area for the period 1963/64-1978/79 (SMHI and FIMR, 1982) and the two dotted curves denote the range of variability.*

saline bottom layer is determined by vertical diffusion and is of the order of 30 years. In addition, the system is forced by intermittent major salt water inflows (Matthäus and Franck, 1992) and by highly variable river discharges (Bergström and Carlsson, 1994). Hence, an average over a 13-year timeslice is not representative for the mean state of the Baltic Sea.

4.1 Sea surface temperature

A map of mean sea surface temperature is shown in Figure 9a. Calculated temperatures range from 5 to $10\,°C$ approximately. The different sub-basins have different mean temperatures showing the influence of the topography on mean horizontal heat fluxes. The temperatures in the Bothnian Bay and Bothnian Sea are around 5 to $6\,°C$, in the Gulf of Finland 6 to $7\,°C$, in the Baltic proper 7 to $9\,°C$ and in Kattegat and southern Baltic 9 to $10\,°C$. Within the Baltic proper a pronounced east-west gradient of about $2\,°C$ is observed. Colder water dominates in upwelling areas close to the Swedish coast and also close to the Finnish coast in the Gulf of Finland whereas warmer temperatures indicate downwelling areas close to the Polish, Lithuanian, Latvian and Estonian coast at the Baltic proper east side. The warmest mean temperatures are related to shallow coastal areas in the Mecklemburg and Gdansk Bight.

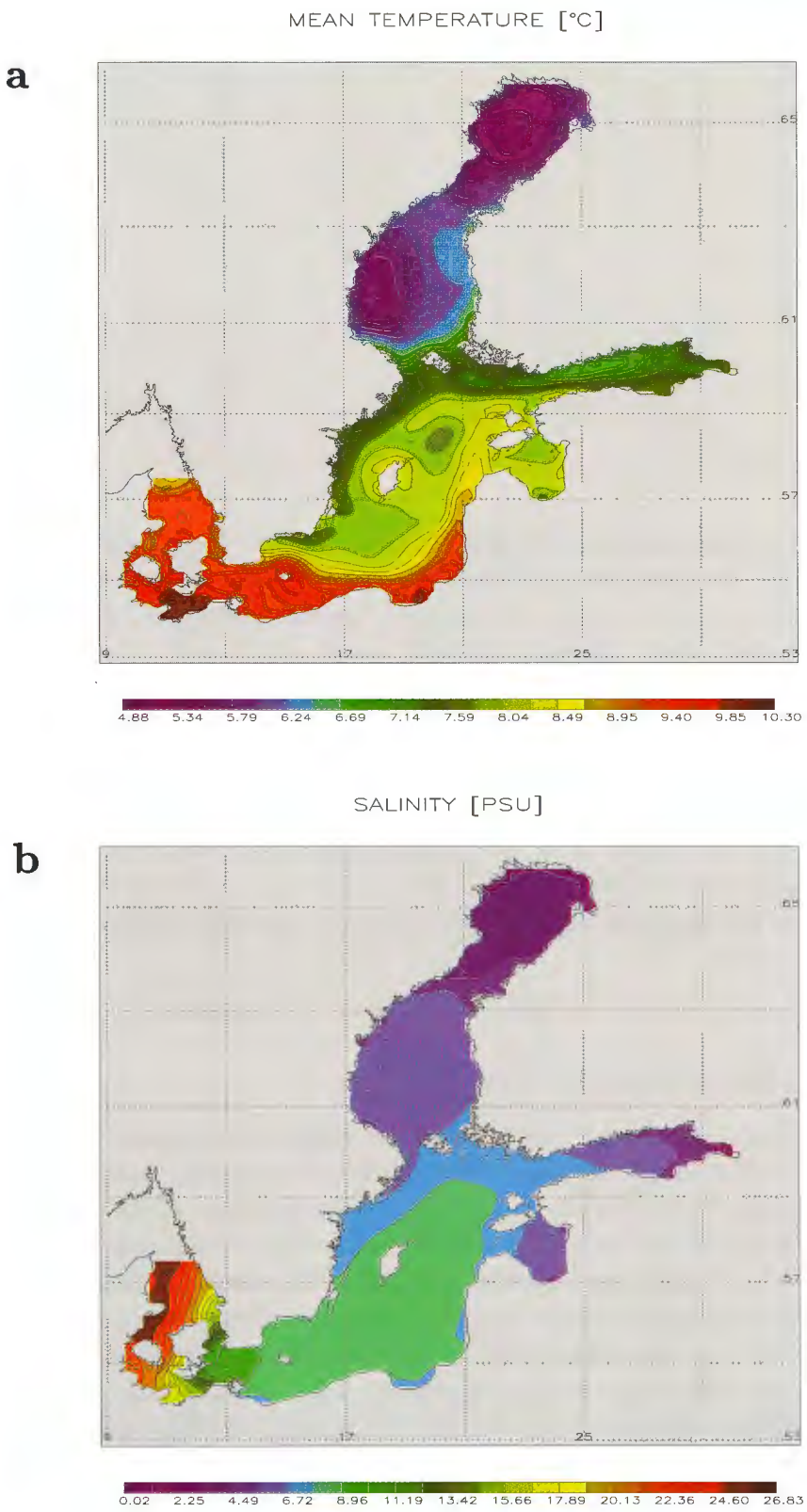

Figure 9: *Mean sea surface temperature (in °C) and salinity (in PSU) for the period May 27, 1980 until May 26, 1993.*

4.2 Sea surface salinity

In Figure 9b mean sea surface salinity is depicted. The salinities range from 0 to $27\,PSU$. At Anholt East in the Kattegat surface salinity amounts to $20\,PSU$ and in the Baltic proper to $8\,PSU$. A strong salinity gradient in Kattegat and in the Danish Sounds marks the border between North Sea and Baltic Sea water. Between the Baltic proper and the Bothnian Bay or the Gulf of Finland salinity decreases to almost zero.

4.3 Temperature and salinity section

In Figure 10 a cross section of mean temperature and salinity through the whole Baltic Sea is depicted. Successively, the section meets Kattegat, Belt Sea with Darss Sill, Arkona Basin, Bornholm Basin, Gotland Deep, Åland Sea, Bothnian Sea and Bothnian Bay. As illustration of the Baltic topography the reader is referred to Figure 3 by Meier et al. (1999). In Kattegat, the western Baltic Sea (Arkona and Bornholm Basin) and in the Gotland Basin the water masses are separated clearly into a homogeneous upper layer and a stratified lower layer as shown in Fig.10b. The outcrop of isohalines at the sea surface in the Belt Sea may indicate the existence of the Belt Sea front which is smeared out in the 13-year mean. The isohalines in the Gulf of Bothnia are weakly inclined and salinity gradients are much smaller. The strongest vertical gradients occur in Kattegat.

Mean temperatures in the western Baltic Sea and in the Gotland Basin reveal a 3-layer structure: warm surface water, cold intermediate water and a bottom layer with moderate temperatures. The permanent thermocline separating the warm surface water from the remaining water body has a decreasing depth from Arkona Basin to the Bay of Bothnia. This surface layer is influenced by the seasonal warming directly. The cold intermediate layer with temperatures between 2 and $4\,°C$ is formed in winter by convection. The saline bottom layer in Bornholm and Gotland Basin has temperatures between 4 and $7°C$.

4.4 Horizontal volume transports

Vertical integrated volume transports (Fig.11a) have typical patterns with only small interannual variability (not shown). Cyclonic cells cover each sub-basin with much smaller transports through the narrow channels connecting the sub-basins which are two orders of magnitude smaller approximately. Maximum mean transports are of the order $10^4\,m^3\,s^{-1}$.

In the vertical the mean current structure differs on different locations (not shown). Figure 11b shows a section across the entrance of the Gulf of Finland in North-South direction (i.e., Finland is to the left and Estonia to the right). At the surface and close to the bottom mean currents are directed into the Gulf of Finland separated by inflowing water in depths between 15 and $40\,m$. Maximum velocities are $1.8\,cm\,s^{-1}$

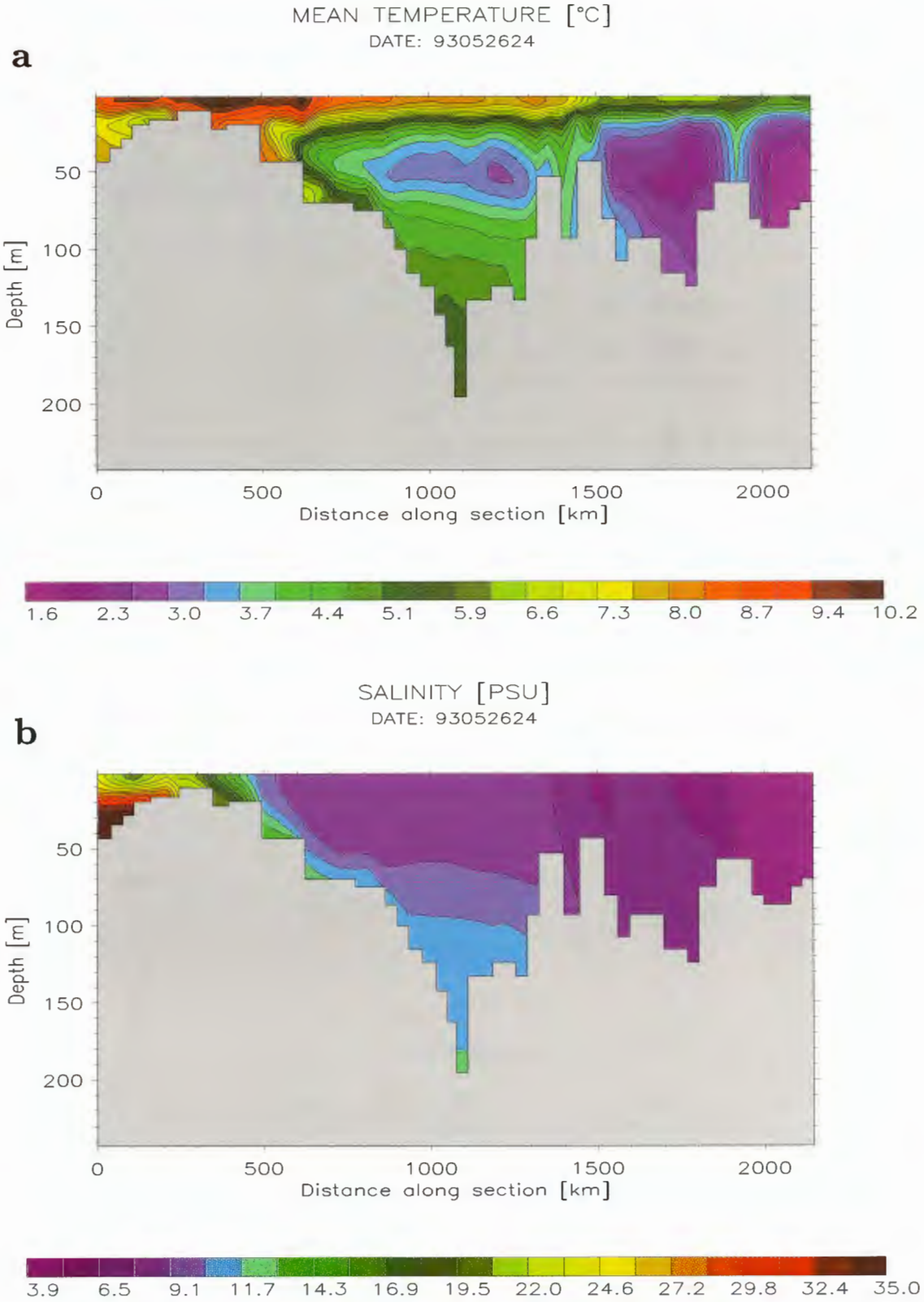

Figure 10: *Mean temperature (in °C) and salinity (in PSU) section through the whole Baltic Sea from Kattegat to Bothnian Bay.*

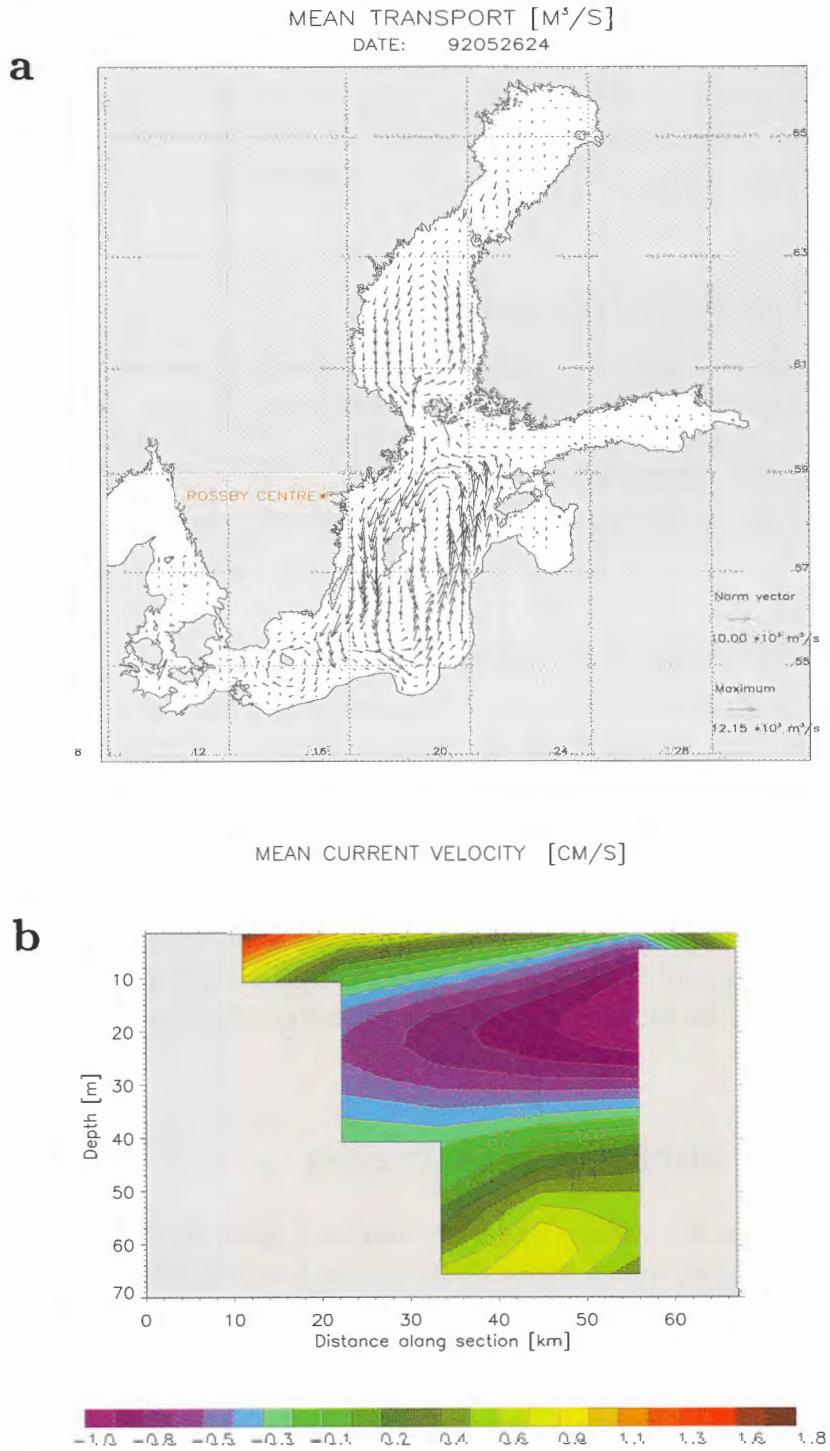

Figure 11: *(a) Mean vertical integrated volume transports for the period May 27, 1980 until May 26, 1992. The amplitude of the depicted norm vector is* $10^4\,m^3\,s^{-1}$. *(b) Mean cross current velocity (in* $cm\,s^{-1}$*) at a North-South section through the entrance of the Gulf of Finland.*

at the surface, $-1.0\,cm\,s^{-1}$ in $20\,m$ depth and $0.7\,cm\,s^{-1}$ at the bottom. This 3-layer structure have been analyzed by the author also in 1 year averages of results from the

Kiel Baltic Sea model (Lehmann, 1995) with a horizontal resolution of $5\,km$. Annual mean velocities in this model vary between $15\,cm\,s^{-1}$ at the surface and $-4.0\,cm\,s^{-1}$ at the bottom. Whether the difference in magnitude between the two models is caused by the different horizontal resolution or by the different averaging period cannot be decided yet. A discussion of the results is given in Section 6.3.

4.5 Horizontal heat transports

Mean horizontal heat transports are distributed similar as the mean volume transports (not shown). Within the Gotland Basin heat is transported from South to North effectively. However, there is no corresponding conveyor belt like in the North Atlantic transporting heat through the whole Baltic from the entrance area to the Bay of Bothnia. The heat transport through the Danish Strait is negligible.

4.6 Ice thickness and concentration

Figure 12 shows mean ice thickness and ice concentration averaged over all seasons of the 13 years. The boundary of mean ice concentration of the simulated period 1980-1993 greater zero agrees well with the climatological average ice extent during a normal winter (Omstedt and Nyberg, 1996). As expected ice concentration and ice thickness are highest in the north-eastern part of the Bothnian Bay and in the eastern part of the Gulf of Finland. Local maxima are found in the narrow channel between Bothnian Bay and Sea (Quark). Local minima of ice concentration occur in the southern central parts of Bothnian Bay and Bothnian Sea. Absolute values are not discussed here because they depend on the summation procedure (in Fig.12 all seasons are included).

5 Mean sea surface heat fluxes

During the integration sea surface fluxes are summed up in RCO every time step for heat and freshwater analysis. A momentum budget has not been considered yet. As the daily cycle is included in the solar radiation model (cf. Section 2.3 by Meier et al., 1999) summation during the model integration is necessary. Snapshots of prognostic ice and ocean variables are written to disk every second day only. The idea behind the heat flux analysis is to calculate closed heat budgets for atmosphere, ice and ocean separately. As outlined below difficulties arise in case of closed budgets for ice and ocean. Hence, the report is focused on a heat budget for the atmosphere.

The total heat flux (Q_{TOT}) from the atmosphere into the coupled ice-ocean system consists of 10 components: shortwave (Q_{SW}), incoming ($Q_{LW\downarrow}$) and outgoing ($Q_{LW\uparrow}$) longwave radiation, sensible (Q_S) and latent (Q_L) heat flux into the ocean and into the sea ice:

$$Q_{TOT} = Q_{TOT}|_{noice}\,(1-c) + Q_{TOT}|_{ice}\,c \qquad (2)$$

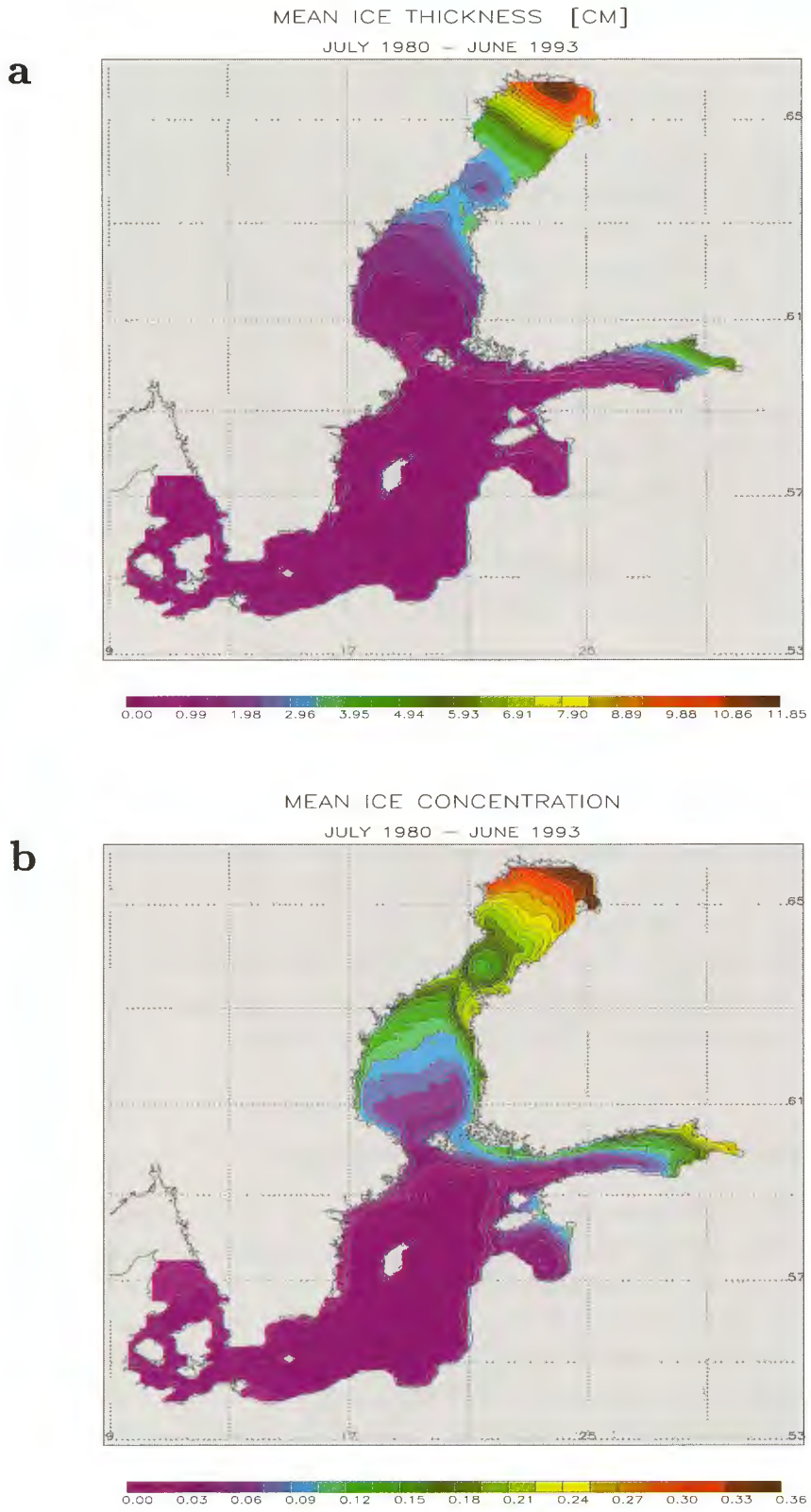

Figure 12: *(a) Mean ice thickness (in cm) and (b) ice concentration for the period July 1980 until June 1993. The average is calculated for the whole period (all seasons).*

with

$$Q_{TOT}|_{noice} = Q_{SW}|_{noice} + Q_{LW\downarrow}|_{noice} - Q_{LW\uparrow}|_{noice} + Q_S|_{noice} + Q_L|_{noice} \cdot \qquad (3)$$

and a corresponding formula for the ice case. The used bulk formulae are given by Meier et al. (1999) in Equation (34), (36), (40), (41), (45), (46) for the ocean and in Equation (102), (103), (104), (105), (107) for the sea ice. During the summation the fluxes into the sea ice must be multiplied with ice concentration c and the fluxes into the ocean with $1 - c$. Thus, atmosphere-ocean heat fluxes in leads are taken into account.

Contrary, a closed heat budget for sea ice is more complex than for the atmosphere. In addition to the 5 flux components at the atmosphere-ice surface one has to consider lateral melting and freezing, solar radiation penetrating the ice Q_{SW}^{ib} (Eq.129), heat storage in brine pockets W_{bri} (Eq.118) and an ice-ocean heat flux Q_{bottom} (Eq.110). According to Semtner (1976) heat flux differences are then used to calculate melting on top of the ice and melting or freezing at the bottom (Eq.115 and Eq.117).

The heat budget for the ocean is calculated from the fluxes at the ice-ocean interface (penetrating solar radiation and ice-ocean heat flux) multiplied with the ice concentration plus the atmosphere-ocean fluxes multiplied with $1 - c$. In case of lateral freezing, all the atmospheric cooling expressed by the volume per unit area of new ice V_{new} is used to close leads. In case of lateral melting however, the heat flux from the atmosphere is divided among lateral melting of ice and warming of water using the ice concentration c (cf. Eq.126 and 128 or Harvey, 1988). Hence, the atmosphere-ocean flux in leads $Q_{TOT}\,(1 - c)$ is zero in case of freezing and is multiplied with a factor $1 - c$ in case of melting to express a decreasing melting effect with increasing ice-free area. As a number of thresholds are necessary for numerical reasons, the explicit calculation of a separate ocean or ice heat budget is quite complicated.

5.1 Net heat fluxes into the atmosphere

Figures 13 and 14 show mean sea surface heat fluxes in RCO averaged for the period June 1980 until May 1993. Positive values indicate fluxes into ice or ocean. In Fig.13a the net heat flux Q_{TOT} between atmosphere and ice/ocean is depicted. Simulated heat fluxes range from -60 to $60\,W\,m^{-2}$. The ocean gains heat from the atmosphere mainly in the northern Bornholm and southern Gotland Basin, in the southern Bothnian Sea and in coastal areas in Kattegat, in the Gulf of Finland close to the Finnish coast and in the southern Gulf of Riga. The ocean looses heat in the eastern and northern Gotland Basin, in the north-eastern Bothnian Sea and in the whole Bothnian Bay. In Gotland Basin the net heat flux is correlated to mean sea surface temperature (cf. Fig.9a) which is caused by northward horizontal heat transport in the ocean and up- and downwelling areas at the coast. The local maximum of net heat loss in the southern Bothnian Bay coincidences with a local minimum of ice thickness and ice concentration (cf. Fig.12) emphasizing the role of sea ice for atmosphere-ocean heat fluxes (cf. Section 6.5 and

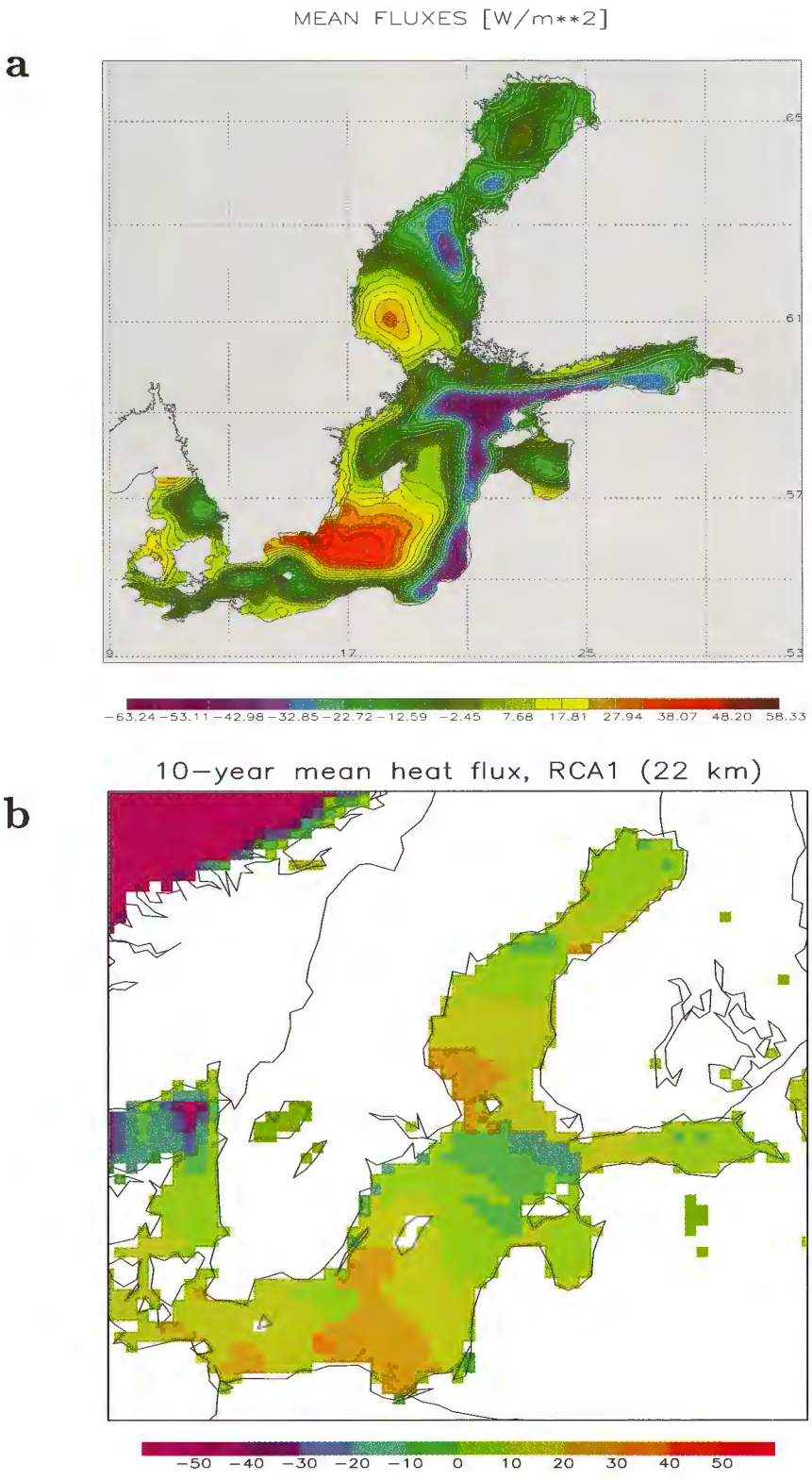

Figure 13: *(a) Mean net heat flux (in W m^{-2}) for the period May 27, 1980 until May 26, 1993. (b) 10-year mean heat flux from RCA1 control run (22 km). Positive values indicate fluxes into ice or ocean.*

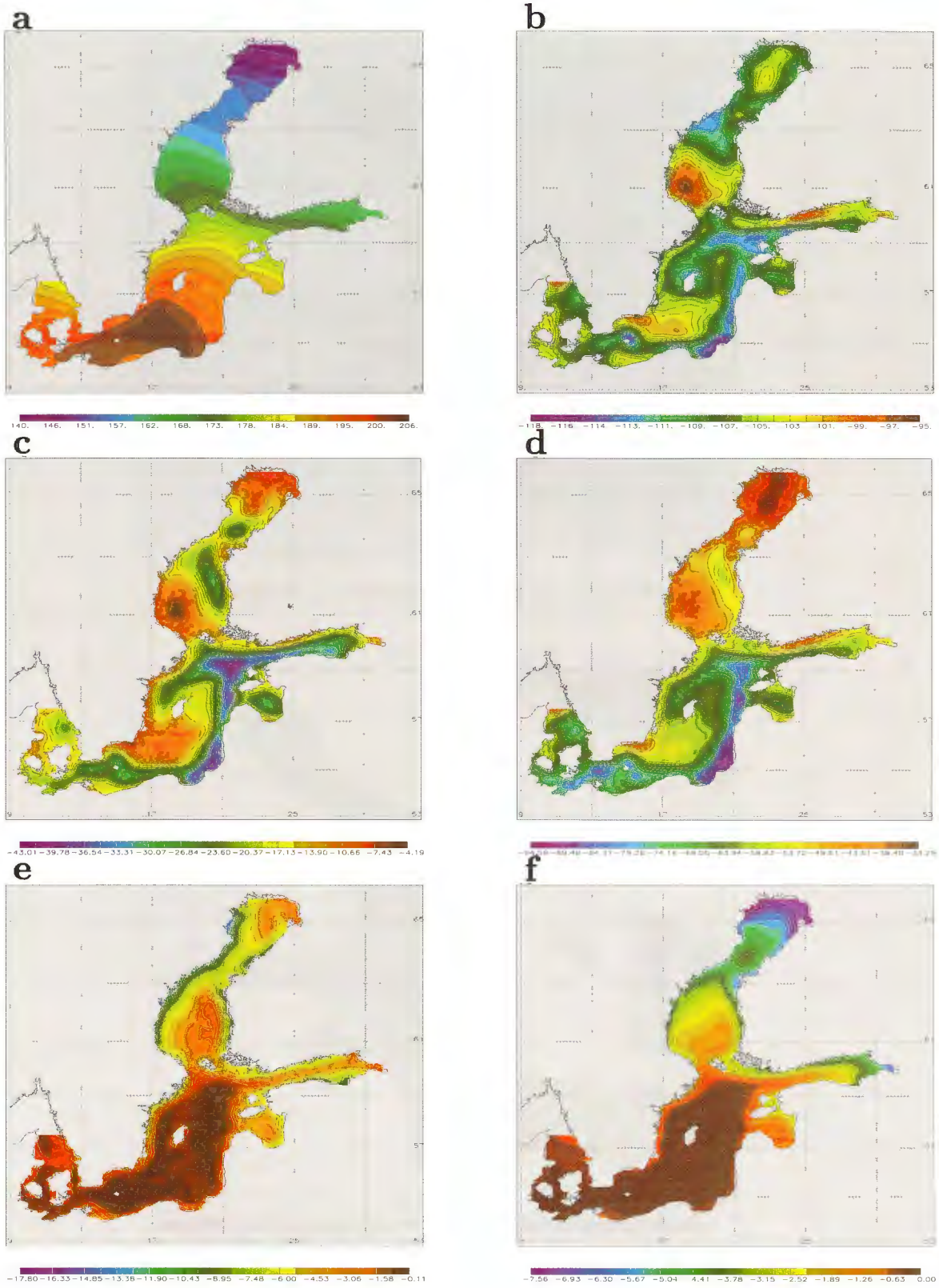

Figure 14: *Mean shortwave radiation (a), longwave radiation (b), sensible (c) and latent heat (d), net heat flux into the ice (e) and flux between ice and ocean (f).*

6.6).

For comparison Fig.13b shows the 10-year mean heat flux in RCA1 control run using the 22 km resolution (Jouni Räisänen, pers.comm.). Version 1 of the Rossby Centre regional Atmospheric climate model, RCA (see e.g., Rummukainen et al., 1998), is coupled with the process oriented, horizontally integrated Baltic Sea model from Omstedt (1990). Boundary data from the global ocean-atmosphere circulation model HadCM2 have been used. The two heat flux maps look somehow similar and the absolute ranges of numbers agree quite well. In RCA1 and RCO 1.0 the Baltic gains/looses heat in the southern/northern Gotland Basin and in the southern/northern Bothnian Sea. Obviously, mean horizontal heat transport from South to North within each sub-basin work similar in both Baltic Sea models.

However, there are also many differing details. The western Baltic Sea (Arkona and Bornholm Basin) looses heat in RCO 1.0 and gains heat in RCA1. The distinct heat loss area in the eastern Gotland Basin related to coastal downwelling does not occur in RCA1. About the reasons only speculations are possible for the moment. Horizontal transports between horizontally integrated sub-basins in the RCA1 ocean model are parameterized and the mean wind-driven circulation (Fig.11) as well as up- and downwelling effects are not included. The latter two processes explain the distribution of mean sea surface temperatures in the Baltic proper as discussed in Section 6.3. Thus, their omission causes different net heat flux patterns. Also different in RCA1 and RCO 1.0 is the net heat flux in Bothnian Bay which is influenced very much by sea ice in general (cf. Section 6.5) and by ice dynamics in special (cf. Section 6.6). The minimum/maximum structure in the two models is reversed.

In RCA1 the heat fluxes of the atmospheric model differ from those of the Baltic Sea model. Different parameterizations and bulk formulae are the reason. Hence, it is not possible to calculate a consistent heat budget for the whole system of atmosphere, ice and ocean. From Fig.13b one can see that areas with positive net heat flux over the Baltic are much larger than areas with negative one. If the Baltic Sea model is using these heat fluxes, it will gain heat from the atmosphere totally and will transport heat through the Danish Straits out of the Baltic. Indeed, this is not the case because the ocean model uses different heat fluxes than depicted. As shown by Omstedt and Rutgerson (1999) Omstedt's model transports only a small amount of heat through the Danish Straits when observed atmospheric forcing is used. The same result is achieved using a 3D model like RCO or the Kiel Baltic Sea model for example. The volume transports through the narrow and shallow channels are too small. Thermodynamically the Baltic Sea can be treated as a lake (Anders Omstedt, pers.comm.). Inconsistent atmosphere-ocean heat fluxes in RCA1 make heat budget calculations impossible.

5.2 Heat flux components

In Figure 14 (a)-(d) the components of net heat flux Q_{SW}, Q_{LW}, Q_S and Q_L are depicted. Thereby, each heat flux is composed of two components. For example the

shortwave radiation is calculated according to

$$Q_{SW} = Q_{SW}|_{noice}\,(1-c) + Q_{SW}|_{ice}\,c\,, \tag{4}$$

whereby the second term is much smaller than the first one. Shortwave radiation is always positive of course and is mainly distributed in latitudinal direction. Net longwave radiation, sensible and latent heat are always negative and show similar patterns than the net heat flux but with local deviations.

Figure 14e shows the net heat flux into the ice neglecting lateral freezing and melting:

$$Q_{TOT}|_{ice} = Q_{SW}|_{ice} + Q_{LW\downarrow}|_{ice} - Q_{LW\uparrow}|_{ice} + Q_S|_{ice} + Q_L|_{ice} - Q^{ib}_{SW} - Q_{bottom}\,. \tag{5}$$

As the mean flux is always negative (out of the ice) the heat budget is not closed for the ice. At the coasts negative values of up to $-18\,W\,m^{-2}$ are calculated whereas in central basins the net heat flux into the ice is almost zero. Obviously, lateral melting contributes significantly in fast ice regions. Further analysis is necessary to elucidate this point.

Figure 14f shows the bottom heat flux between ice and ocean Q_{bottom} (positive into the ocean). This flux must be always negative because sea surface temperature is limited by freezing point temperature. Thus, the ice gains always heat from the ocean. The pattern is highly correlated with the mean ice concentration distribution (cf. Fig.12b).

5.3 Mean seasonal cycle of heat fluxes

Simulated mean seasonal cycles for surface heat fluxes into the atmosphere and out of the sea ice are shown in Figures 15 and 16, respectively. The budgets are calculated according to Equation (2) and (5). During ice growth in winter net longwave radiation is large causing a net heat flux out of the ice (Fig.16). In spring the shortwave radiation gets more and more important. Thus, net heat flux is directed into the ice causing ice melt.

5.4 Time series of heat fluxes

After the presentation of annual mean and seasonal mean heat fluxes in RCO in previous subsections Figure 17 shows now records of horizontally integrated heat fluxes into the atmosphere to give an impression of interannual variability of heat fluxes. The net heat flux amplitude varies by almost a factor of two between different years ($\pm 200\,W\,m^{-2}$ to $\pm 400\,W\,m^{-2}$).

6 Sensitivity and process oriented studies

As outlined in the introduction sensitivity and process oriented studies have been performed and analyzed. Here, a selection of these experiments is presented.

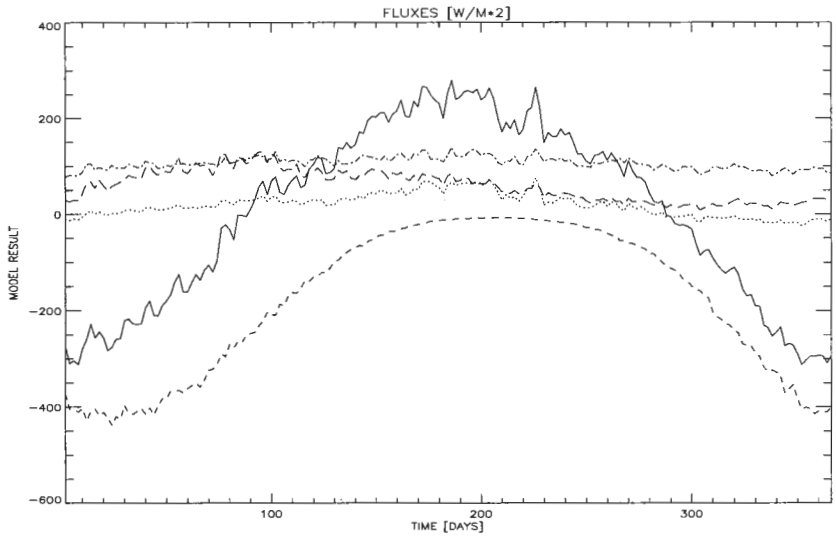

Figure 15: *Mean seasonal cycle of surface fluxes (in W m^{-2}) into the atmosphere from June until May of the following year. Positive values indicate heat fluxes into the atmosphere (solid: net heat flux, dashed: shortwave radiation, dashed-dotted: longwave radiation, dotted: sensible heat, long-dashed: latent heat).*

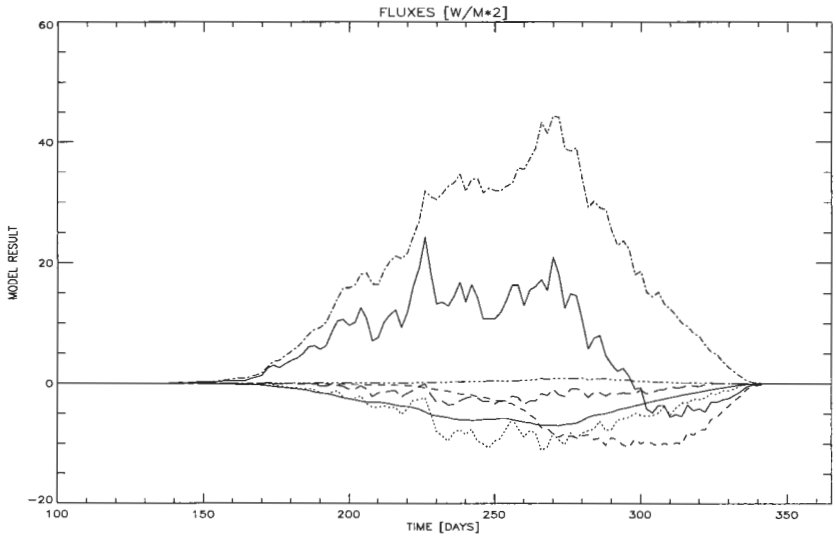

Figure 16: *The same as Fig.15 but mean fluxes into the ice. Positive values indicate heat fluxes out of the ice. In addition to Fig.15 the ice-ocean heat flux (solid, always negative) and the shortwave radiation penetrating the sea ice (dashed-dotted with 3 dots, always positive) is shown. Note that the time axis is reduced (start after 100 days).*

6.1 Advection scheme

The horizontal and vertical advection scheme in RCO 1.0 is the same as in OCCAM (Webb et al., 1998). The advection operator can be splitted into a term of central differences and a velocity dependent biharmonic diffusion term. The diffusion term is used to correct wave dispersion of the central differences. Dispersion causes narrow maxima to be reduced in amplitude and to be broken up into shorter wavelength noise.

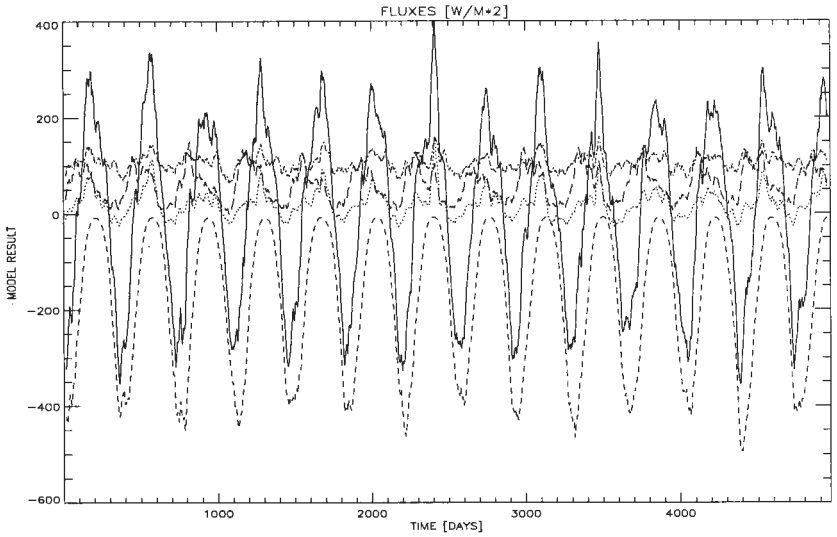

Figure 17: *Horizontally integrated heat fluxes into the atmosphere (positive) for the period May 27, 1980 until May 26, 1993. The meanings of the curves are the same as in Fig.15.*

The use of the improved advection scheme leads to a better representation of mesoscale physics as shown by Webb et al. (1998) but has the disadvantage to introduce numerical diffusion which affects long-term integrations. In the present simulations using RCO the differences between improved advection and central differences at Gotland Deep are of the order $0.5\,PSU$ (not shown). Depending on the application one has to decide whether phase speed of waves or background diffusivity has to be modeled correctly. Nevertheless, the numerical diffusion is much smaller than physical based mixing within the halocline, which is probably caused by breaking internal waves and needs to be parameterized explicitly.

6.2 Open boundary conditions

In Section 3.2 results of isohaline depths at Bornholm deep have been shown with too low salinity in the bottom layer after about 1000 days of integration. These results are received using a climatological profile from Anholt East at the northern boundary in Kattegat calculated from observations of the period 1980-1993. In case of inflow, temperature and salinity at the boundary is relaxed towards these stationary climatological data. This simplification is not critical for temperature but for salinity. The open boundary is located in an area of highly variable horizontal salinity gradients in time, the Kattegat-Skagerrak front (Jakobsen, 1997). To show the sensitivity of the Baltic Sea interior from open boundary conditions an experiment has been performed with increased salinity in the upper layer. Instead of the climatological value of $20\,PSU$ $25\,PSU$ has been used in the sensitivity experiment. The results for Bornholm Deep are shown in Figure 18. Compared to Fig.3b (same colour bars) salinity in the deep layer is increased. The salt water inflow is now simulated with bottom salinities of more than $18\,PSU$ which is close to observations. Other inflows during the integra-

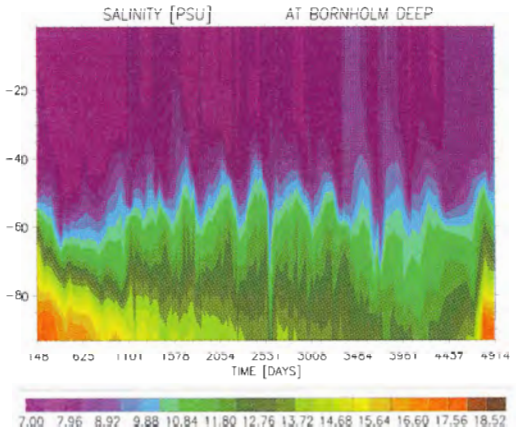

Figure 18: *Simulated isohaline depths (in PSU) from May 1980 until June 1993 at Bornholm Deep with changed boundary conditions in Kattegat. The counting of days start at January 1, 1980.*

tion period are still underestimated but the results are improved. It is not realistic to have the increased salinity at the northern model boundary prescribed all the time. However, it is important simulating larger salt water inflows to take the movement of the Kattegat-Skagerrak front into account. During the inflow event in January 1993 it was estimated that 310 km^3 water crossed Darss and Drogden Sill (Matthäus et al., 1993) within 21 days (Meier, 1996). This water originates from Belt Sea and Kattegat. According to Stigebrandt (1995) the volume of Kattegat surface water amounts to 275 km^3. Hence, it is concluded that water from outside the model domain must have passed the Sills in the Danish Straits during the inflow. Time dependent salinity profiles at the open boundaries or a larger model domain as planned for the next version of RCO will improve the long-term behavior of deep water salinity in Bornholm Basin.

In addition, the coarse horizontal resolution of 6 nautical miles causes problems with overflows which are typical for level models (Beckmann and Döscher, 1997). Meier et al. (1999) have shown that the results for RCO will improve at least for the salt water inflow in 1993 if a horizontal resolution of 2 nautical miles is used.

6.3 No Wind

The distribution of mean sea surface temperatures as shown in Figure 9a is explained by the North-South gradient of mean air temperatures as well as by the dynamic effect of the ocean. Switching off the wind forcing completely results in only latitudinal dependent distribution of SST's (Fig.19a). The cyclonic cells of vertical integrated volume transports disappear and maximum transports are now 3 times smaller (Fig.20). It should be noted that these transports are not identical with the pure thermohaline driven circulation because the sea level forcing in Kattegat is still active causing volume

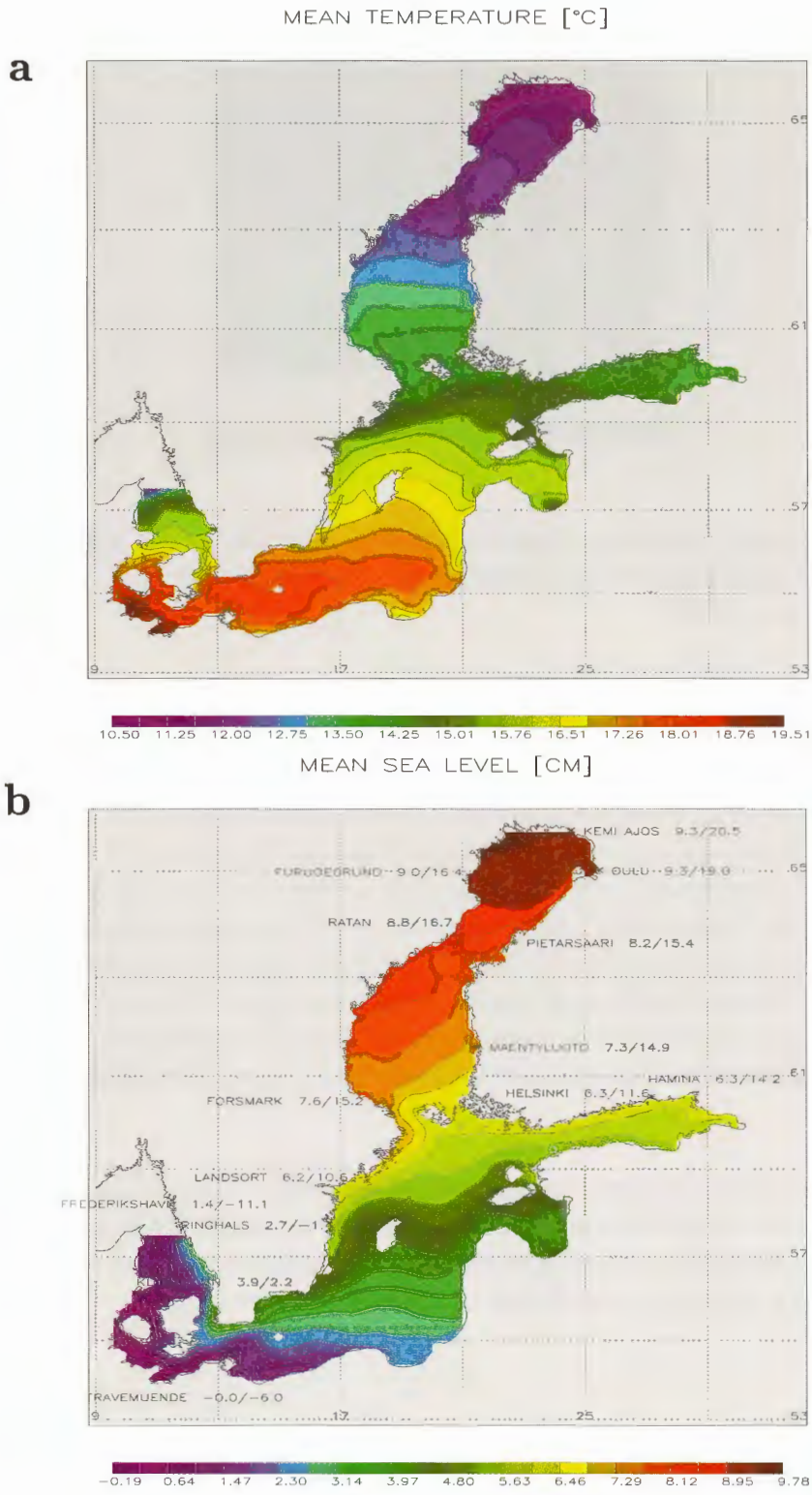

Figure 19: *(a) Mean sea surface temperature (in °C) and (b) sea surface height (in cm) for the period May 27, 1980 until May 26, 1993 (May 26, 1992 in case of (b)). The numbers at selected tide gauge positions indicate model results (left) and geoid solutions of Ekman and Mäkinen (1996) (right). In this simulation no wind forcing is used.*

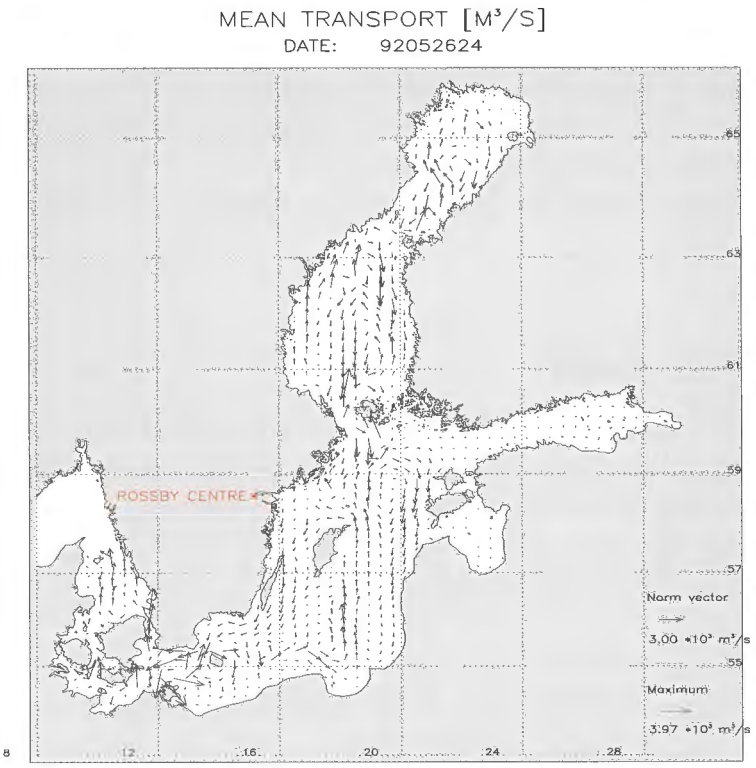

Figure 20: *Mean vertical integrated volume transports (in* $10^4\, m^3\, s^{-1}$*) for the period May 27, 1980 until May 26, 1992. In this simulation no wind forcing is used.*

changes in the Baltic on monthly and longer timescales. Hence, corresponding mean transports overlay the thermohaline residual circulation.

The mean wind-driven horizontal circulation changes also vertical momentum balances. Mean wind speed causes a mean Ekman transport to the right of the wind direction. As the mean wind direction is from South-West mean Ekman transport causes inflow at the surface into the Gulf of Finland (Fig.11b). The cross section through the entrance of the Gulf of Finland show an inflow of water from the Gotland Basin into the Gulf of Finland at the surface, outflow of lower saline water in intermediate depths and inflow of higher saline water close to the bottom.

Without mean wind effect the estuarian vertical circulation would only consist of outflow of low saline water in the upper layer and inflow of high saline water at the bottom (e.g., Welander, 1974). Consideration of the mean wind effect results now in a 3-layer structure. If mean wind speeds are not overestimated the traditional view of a purely two layer transport system needs to be revised. The overestimation of simulated sea surface heights in the Gulf of Finland (about $7\,cm$ at Hamina, cf. Fig.4) indicates that indeed the mean wind speeds might be too high.

Figure 19b show the 13 year mean sea surface height without wind forcing. Compared to Figure 4 the sea level in the Bothnian Bay (Kemi, Oulu) drops from 22 to $9\,cm$ and in the Gulf of Finland (Helsinki, Hamina) from 19/21 to $6\,cm$. This is remarkable

because the initial stratification has not been changed. Although the mean wind speed in the atmospheric forcing data set might be too high, only with wind effect included the geoid solution of sea surface heights are reproduced by the model. Without mean wind speed the observed sea levels are underestimated by a factor of two approximately. Hence, a mean 3-layer transport structure in the entrance of the Gulf of Finland might be realistic.

6.4 Increased runoff

The first scenario experiments of the Rossby Centre indicate higher precipitation and river runoff in the future. The change in average annual runoff between RCA0 control and scenario run from HBV-Baltic are 21 % for the Bothnian Bay, 14 % for the Bothnian Sea, 22 % for the Gulf of Finland, 31 % for the Gulf of Riga, -4 % for the Baltic proper and 12 % for the total Baltic Sea area (Phil Graham, pers.comm.).

To show the principal effect of increased river runoff without the aim to perform a realistic scenario for the Baltic Sea river runoff has been increased by 50 % for all rivers. The sea surface heights increase then by only less than $1\,cm$ (not shown). At Gotland Deep (Fig.21a, b) the salinity in the surface layer decreases whereas the lower layer salinity does not change. The changes are greatest in the upper part of the halocline ($1\,PSU$ after about 5000 days of integration) and smaller close to the surface ($0.5\,PSU$). These differences reflect the deepening of the halocline.

Results for Bornholm Deep are shown in Figure 21 (c) and (d). In Bornholm Basin the situation is reversed compared to Gotland Basin. The salinity of the deep water decreases by more than $1.5\,PSU$ whereas surface salinity is less affected by the increased river runoff ($< 0.5\,PSU$). Especially, during the inflow event in January 1993 the bottom salinity increase is more than $2\,PSU$ smaller. Increased river runoff affects the water exchange through the Danish Straits tremendously in blocking the inflow of high saline water from Kattegat into the Baltic Sea.

6.5 No sea ice

Sea ice in the Baltic is regarded as a key element in the North-European climate system because it acts as a relatively rigid insulating film between the air and the sea which modifies air-sea exchange of momentum, heat and matter and influences local meteorological conditions. The importance of the albedo feedback cannot be emphasized too often. With respect to the ocean sea ice influences the temperature and salinity characteristics of the water masses and the circulation of the Baltic Sea. In the following it will be discussed how mean sea surface temperature, mean sea surface height and mean net surface heat flux are affected by sea ice.

Figure 22 shows mean SST (a) and SSH (b) difference between experiments with and without sea ice for the whole 13-year period (averages include also summer time). In

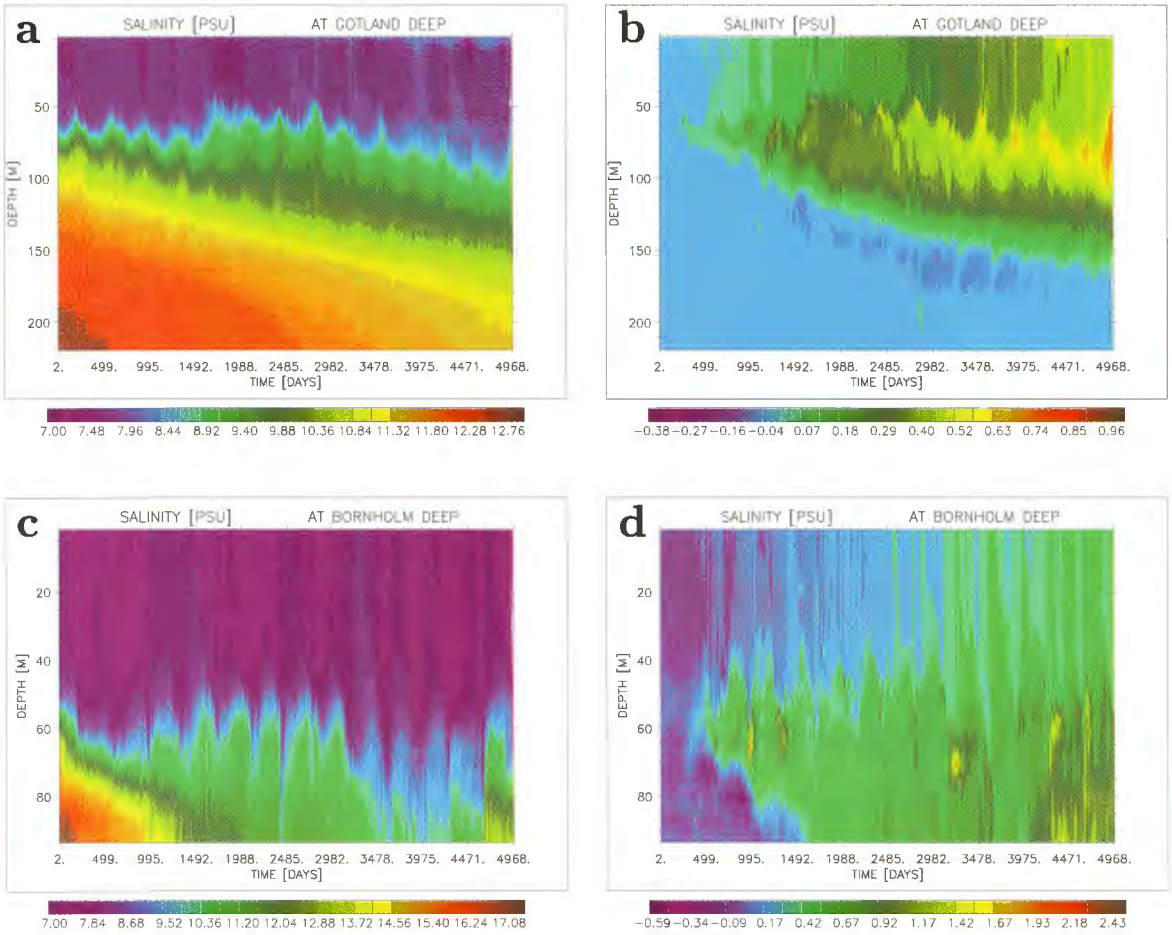

Figure 21: *Simulated isohaline depths (in PSU) from May 1980 until December 1993 at Gotland Deep with increased runoff (a). (b) shows the difference between experiments with present day (Fig.2c) and 50 % increased runoff. Results for Bornholm Deep are depicted in (c) and the corresponding difference in (d). The counting of days start at May 26, 1980.*

the simulation without ice temperatures are limited by freezing point temperature simply. With ice mean sea surface temperatures in the central parts of the Bothnian Sea and Bothnian Bay are systematically higher with up to $0.25\,°C$. Shallow coastal areas are colder with up to $-0.33\,°C$.

The effect of sea ice on mean sea surface height is small (Fig.22b) compared with basin-wide gradients (Fig.4). In coastal areas of the Gulf of Bothnia and Finland mean sea surface height is about $1\,cm$ lower with sea ice than without. The difference over the whole model domain is always negative as expected. Zhang and Leppäranta (1995) have modeled the influence of ice on sea level variations in the Baltic Sea for 3 study cases each covering a period of 120 hours. They have shown that the water piling-up with ice is decreased to one-third and that for severe ice conditions the current field magnitude dropped to 20 % from the ice-free case. Further studies are necessary to show whether the small effect on the 13-year mean ssh is caused by the long averaging interval or by a shortcoming of the present RCO version.

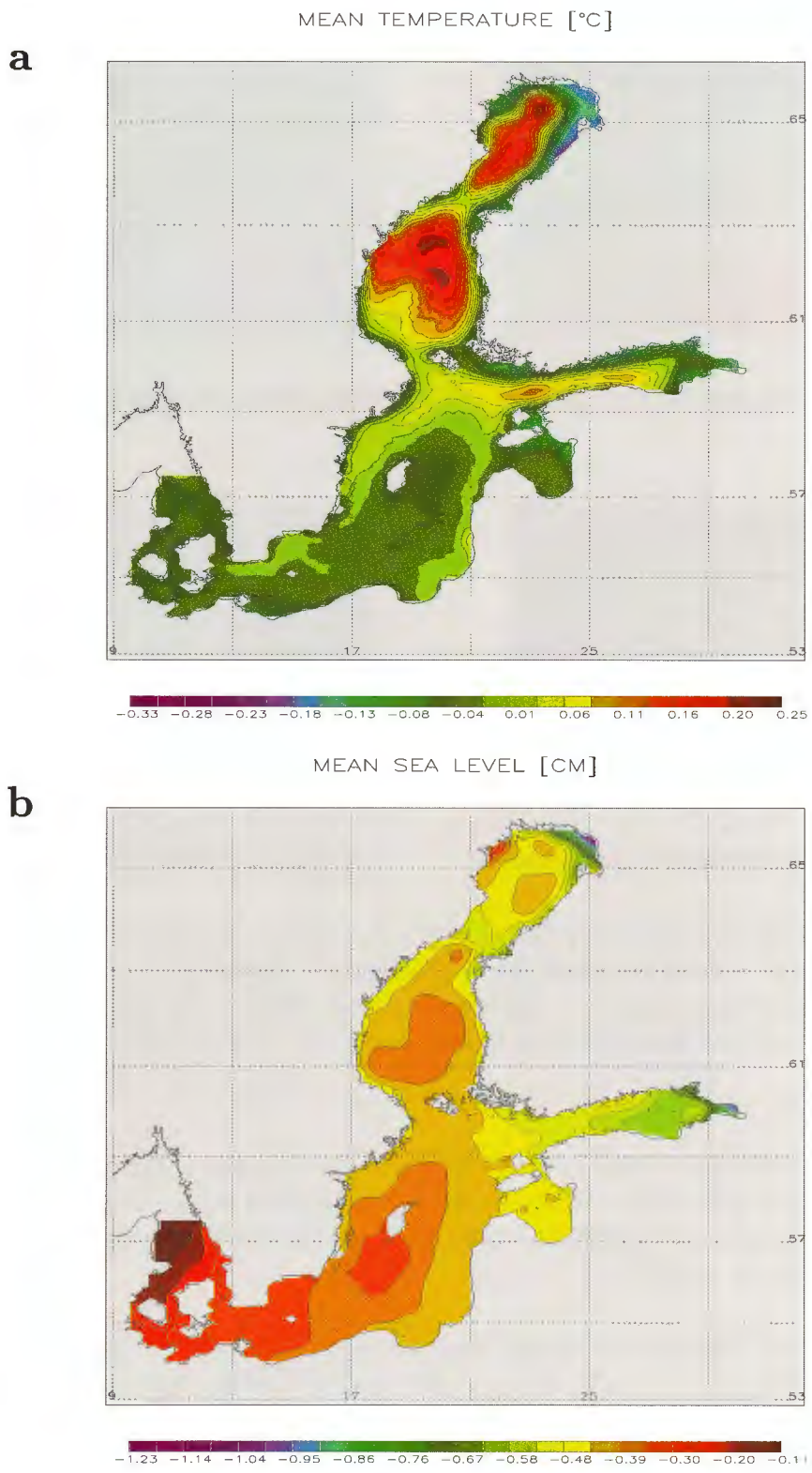

Figure 22: *(a) Mean sea surface temperature difference (in °C) and (b) sea surface height difference (in cm) between experiments with and without sea ice for the period May 26, 1980 until May 25, 1993.*

Although the effect of ice on mean sst's is relatively small (compared to the case when temperatures are limited by freezing point temperature), the effect on mean net surface heat flux is tremendous (Fig.23a). The difference in mean heat loss for the northern parts of the Baltic Sea is greater than $90\,W\,m^{-2}$ and is of the order of the absolute range of horizontal net heat flux variations (cf. Fig.13). The heat flux difference pattern is highly correlated to mean ice concentration (Fig.12).

6.6 No ice dynamics

Within the SWECLIM project a decision had to be made which sea ice model to use. A SWECLIM workshop on coupled ice-ocean models for the Baltic Sea has been held in November 1998 (Meier, 1998). The workshop was intended to address the problems of different approaches. Among others the question has been discussed if it is really necessary to include ice dynamics into the coupled atmosphere-ice-ocean system to be developed for multi-year integrations. Problems with the parallelization of the traditionally used algorithms for dynamical sea ice models with viscous-plastic rheology according to Hibler (1979) have been expected. Due to the experience from operationally running models for ice forecasting advection and dynamics of ice are important in the Baltic Sea (e.g., Matti Leppäranta, pers.comm.). Hence, it has been decided to use the ice model with elastic-viscous-plastic rheology from Hunke and Dukowicz (1997). The constitutive law has been changed adding artificial elastic waves for numerical reasons. This modification leads to a fully explicit numerical scheme that further improves the model's computational efficiency and is a great advantage for implementations on parallel machines (Hunke and Zhang, 1999). In Meier et al. (1999) it has been shown that the elastic-viscous-plastic sea ice model performs well also for Baltic ice conditions. A process study from the beginning of February 1993 showed that under strong wind conditions a hole in the ice coverage can open with the size of half of the Bothnian Bay. This phenomenon can be modeled only with ice dynamics included.

Now the question arises whether ice dynamics affects also 13-year mean ice thicknesses, ice concentrations and net surface heat fluxes. Hence, a comparison between an experiment with full dynamic-thermodynamic ice model and one without dynamic effects ($\vec{u}_{ice} = 0$) has been performed. Figure 24 shows the difference for ice thickness and ice concentration. The mean wind field from south-westerly directions causes higher ice thicknesses and ice concentrations in the north-eastern parts of the Bothnian Bay and in coastal areas of the eastern Bothnian Sea and northern Gulf of Finland. Less ice thicknesses and concentrations are found in the western and southern parts correspondingly. About half of the mean ice thickness at the northern end of the Bothnian Bay (e.g., at the location Kemi) is explained by the dynamical effect (cf. Fig.12a). Ice concentration is affected by 17 % (cf. Fig.12b). The local minimum in ice thickness and concentration in the southern Bothnian Bay (north of the Quark) is mainly caused by ice dynamics. Only a weak minimum occur in the dynamic-free case (not shown).

The sensitivity of ice concentration has an effect on the net heat flux as shown in Figure 23b and on the flux components as shown in Figure 25. With ice dynamics the net heat

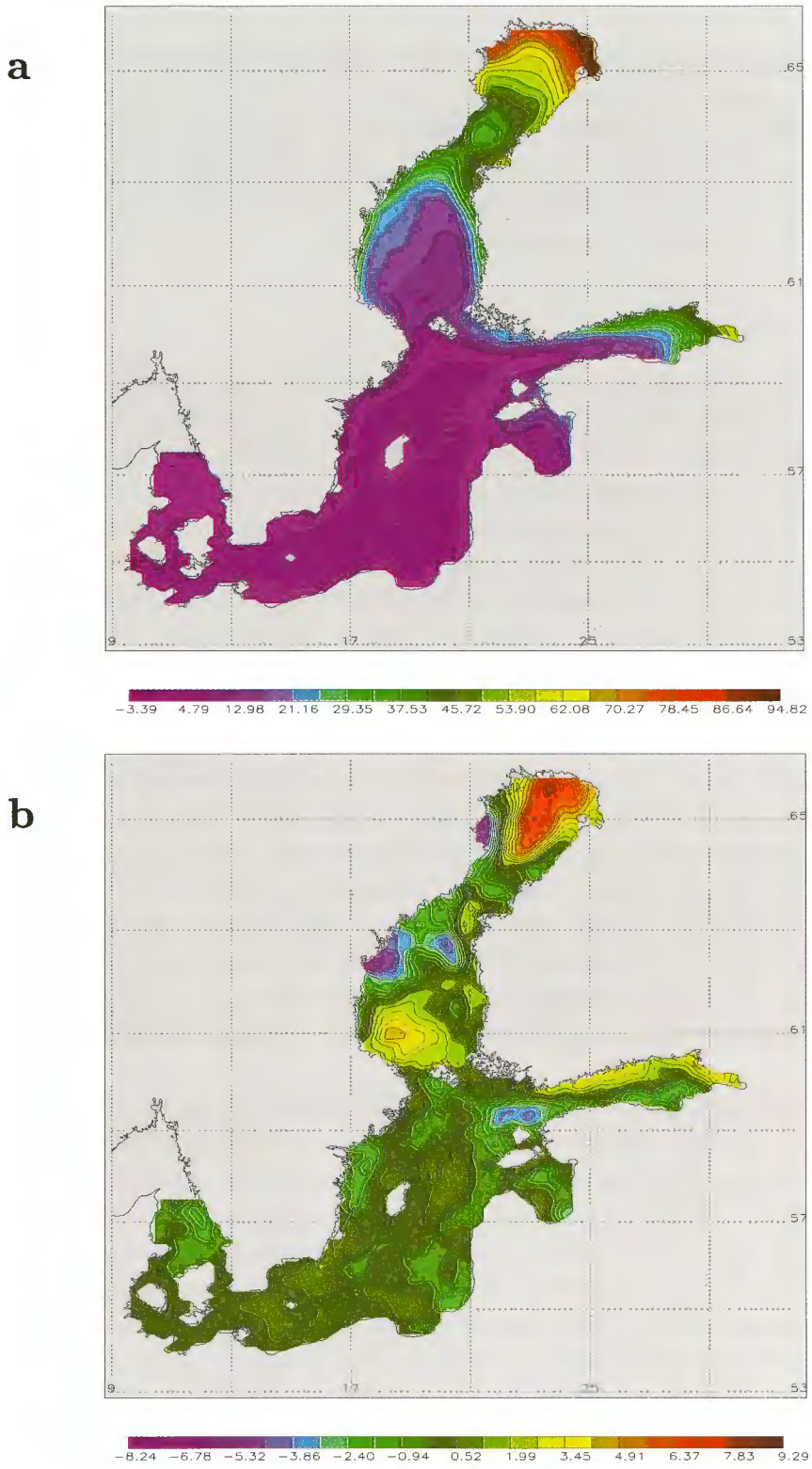

Figure 23: *Mean heat flux difference (in $W\,m^{-2}$) between experiments with and without sea ice (a) and between experiments with and without ice dynamics (b) for the period May 26, 1980 until May 25, 1993.*

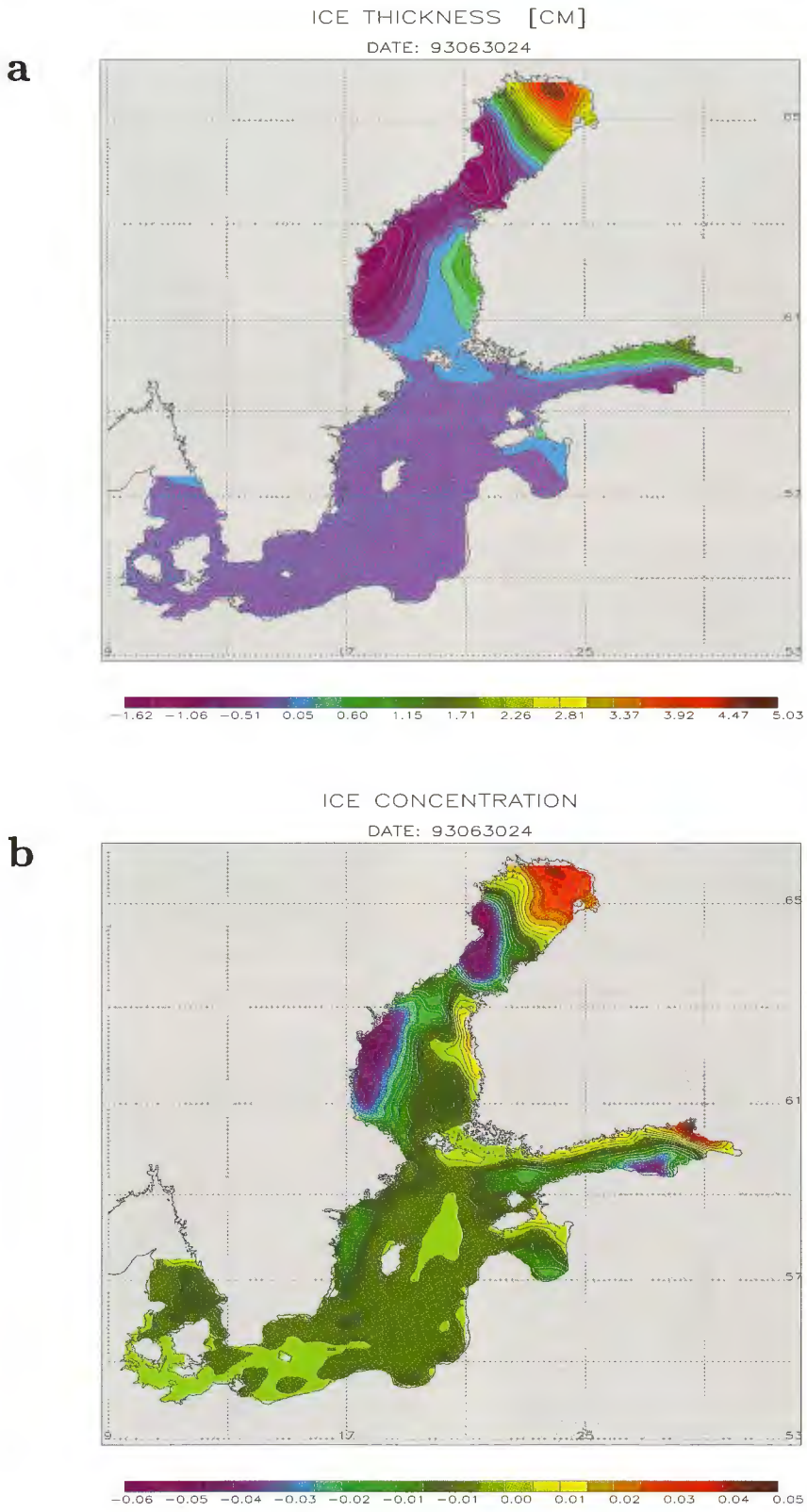

Figure 24: *(a) Mean ice thickness (in cm) and (b) ice concentration difference between experiments with and without ice dynamics.*

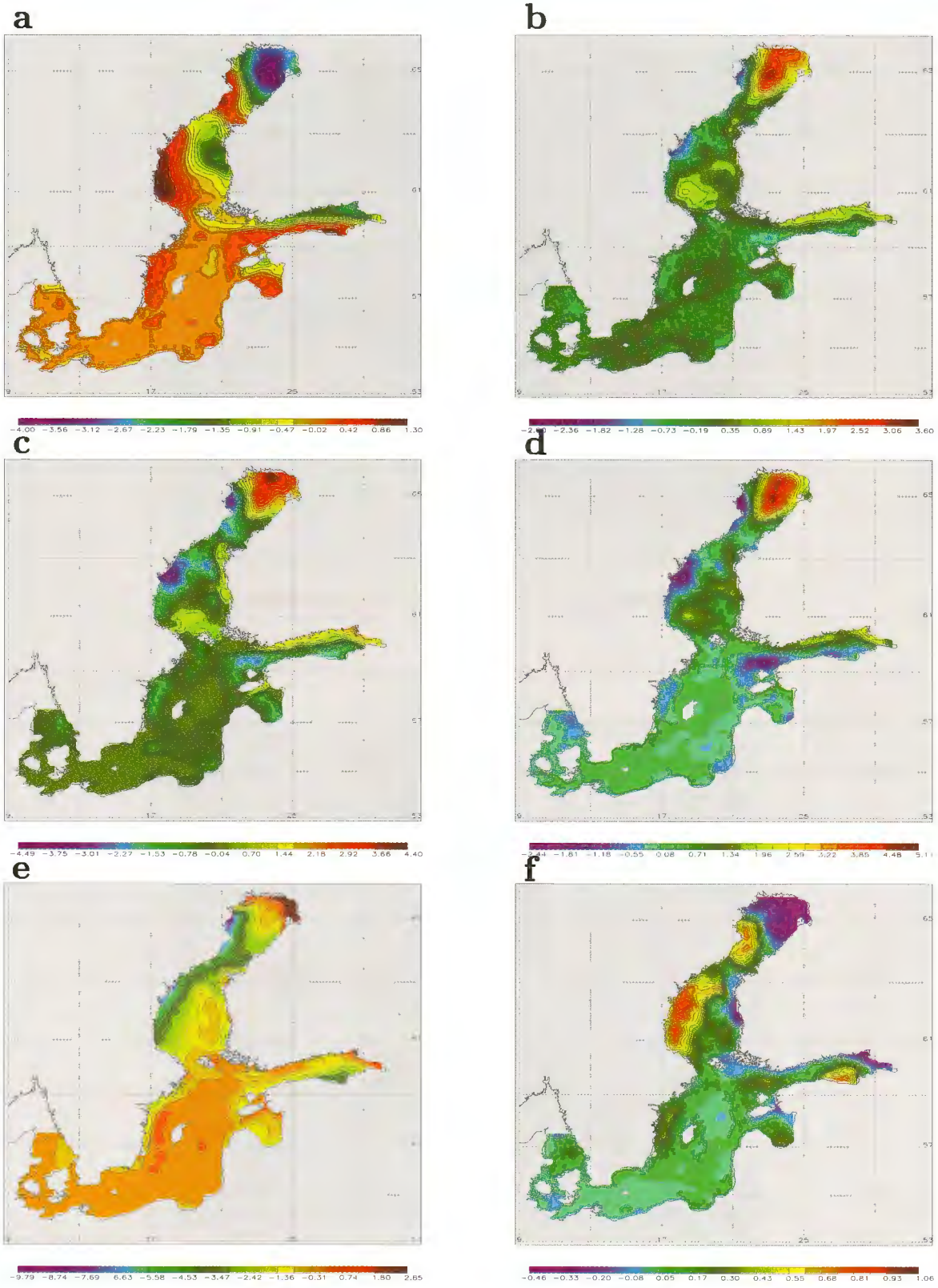

Figure 25: *Heat flux differences between experiments with and without ice dynamics (a: shortwave, b: longwave, c: sensible, d: latent, e: net ice, f: ice to ocean, cf. Fig.14).*

loss in the central and northern Bothnian Bay is reduced by $9\,W\,m^{-2}$ but enhanced in the western Bothnian Bay and north-western Bothnian Sea by $8\,W\,m^{-2}$ approximately. The heat gain in the southern Bothnian Sea is about $5\,W\,m^{-2}$ greater with ice dynamics than without. Similar horizontal difference patterns are found for longwave radiation, sensible and latent heat (Fig.25b, c, d). Shortwave radiation (Fig.25a) is very much correlated with mean ice concentration (Fig.24b). Higher ice concentration causes higher albedo and lower solar insolation into the ice/ocean.

The net heat flux out of the ice (Fig.25e) in coastal waters of the western Bothnian Bay and Bothnian Sea is maximum $10\,W\,m^{-2}$ higher with ice dynamics than without. The largest outgoing net ice fluxes in the full ice model are $-18\,W\,m^{-2}$ (Fig.14e) but only $-12\,W\,m^{-2}$ in the ice dynamic-free case (not shown). The latter flux pattern is rather symmetric with respect to eastern and western coastal waters.

As expected the bottom heat flux between ocean and ice is lower in the western and higher in the eastern parts of the mean ice covered area (Fig.14f).

7 Summary

Simulations of the hindcast period 1980 until 1993 have been performed using a coarser grid version of RCO (6 nautical miles). In Meier et al. (1999) the model has been described and tested for one particular year, 1992/93. In this report now the integration period has been extended to more than 13 years (1980-1993). RCO has been developed within SWECLIM for 10-year timeslice experiments of climate change scenarios. To get confidence in the model results and to determine uncertainty ranges it has been decided that the step before the scenario simulations needs to be an intensive model-data comparison for hindcast experiments. From observed temperature and salinity profiles initial conditions have been generated. Realistic atmospheric forcing and river runoff have been used. The results of 13 year long simulations have been compared to monitoring profile data of the SHARK data base, mean sea surface height, ice extent and ice thickness data.

The seasonal cycle of the thermocline in different sub-basins is simulated satisfactory. There is slight underestimation of mixed layer depth only in some years indicating inaccuracy of the atmospheric forcing data. Artificial trends are not observed.

Time evolution of the halocline in the Baltic proper during the stagnation period between 1980 and 1992 is simulated realistically. Due to carefully chosen parameterizations erosion of the halocline could be avoided. Only a slight drift of sea surface salinity indicate the need of further improvements with respect to the interaction of turbulence with stratification for example. The successful simulation of more than 10 years represent a milestone progress because exactly this feature was unclear a year ago. Within SWECLIM a parallel 3D Baltic Sea model with sea ice included is now available to perform long-term simulations. To the authors knowledge this model is unique for the Baltic Sea.

Deep water mixing has been added successfully. However, there is evidence from observations (seasonal cycle, mixing depends on coastal distance) and from model results (divergence of isohalines in the upper halocline) that the parameterization of deep water mixing needs to be improved.

The problem of coarse resolution level models with overflow is visible in results from Bornholm Basin. Salt water inflows from Kattegat into the Baltic Sea are underestimated resulting in too strong decrease of bottom layer salinity after about 1000 days of integration. In addition, larger salt water inflows are affected by shortcomings of the open boundary conditions in Kattegat of the present RCO version. Due to the lack of time dependent observations climatological data have been used which are not suitable to simulate the movement of the Kattegat-Skagerrak front. Hence, water with too low salinity is transported through the Danish Straits during inflow events. Increased horizontal resolution, a bottom boundary layer model as described by Döscher and Beckmann (1999) and a larger model domain will help to overcome these problems in the next RCO version already under preparation.

The agreement between simulated mean sea surface heights and geoid results is very good. About 50% of the sea level difference between Kattegat and Bothnian Bay is explained by the mean wind effect. Even more important seems to be mean wind for sea surface heights in the Gulf of Finland. Mean wind speeds from south-westerly directions cause a cyclonic horizontal circulation in each sub-basin. It has been shown that this mean wind-driven circulation affects vertical balances. For example in the entrance area of the Gulf of Finland a 3-layer transport system is established. Contrary, process oriented models developed for Baltic Sea climate research are based on a 2-layer transport approach. So far, it has been assumed that mean Ekman transport is unimportant and consequently has been neglected.

The ice model within RCO predicts maximum ice extent and ice thicknesses at Kemi in the Bothnian Bay quite well. However, during mild winters ice extent is overestimated and ice thickness underestimated slightly. Contrary, ice thickness is overestimated during severe winters. The analysis of Kemi data might be misleading because only one coastal station cannot determine the model performance of simulated horizontal ice thickness distributions. Further analysis of ice thickness and ice concentration is still necessary.

The comparison of simulated mean time evolution of relative ice cover with data from the Ice Atlas needs to be reviewed carefully as the two periods under investigation are different. Under the assumption of same statistics (which is not true) mean time evolution and variability are simulated correctly but ice melt in spring is predicted too early.

Selected mean ice/ocean variables (i.e., SST, SSS, SSH, temperature and salinity cross sections, volume transport, ice thickness and ice concentration) and mean sea surface heat fluxes (net and components) are presented and discussed. Net heat fluxes in RCO 1.0 and RCA1 are compared. The overall heat flux patterns are similar but local differences occur which might be explained by the two different approaches of used Baltic Sea models. In RCA1 the heat fluxes for the atmosphere are not consistent with those for the ocean emphasizing the need to develop a fully coupled atmosphere-ice-ocean system.

A set of sensitivity and process oriented studies have been performed to increase our understanding of the processes involved:

- An experiment without wind forcing points out the importance of mean wind speed for mean sea surface height and mean circulation.
- 50 % increased river runoff causes deepening of halocline depth in Gotland Basin and freshening of surface water salinity by $0.5\,PSU$. Contrary, in the western Baltic (e.g., Bornholm Basin) mainly the lower layer salinity is affected. Increased river runoff causes blocking of inflowing salt water through the Danish Straits.
- Without ice net heat loss in seasonal ice covered areas are increased tremendously showing the important isolating effect of ice.

- Consideration of ice dynamics results in higher/lower ice thickness and ice concentration in the eastern/western parts of the Gulf of Bothnia. Correspondingly, mean heat flux patterns are affected.

In addition to necessary model improvements future activities will concentrate on exploring uncertainty ranges. Different atmospheric forcing (ECMWF re-analysis data) and different bulk formulae for heat fluxes will be used in hindcast experiments (1980-1993). A systematic sensitivity study as performed by Simonsen and Haugan (1996) for the Arctic Ocean and Nordic Seas is under preparation for the Baltic Sea.

Acknowledgments

The SWECLIM program and the Rossby Centre are funded by MISTRA and by SMHI. The testing and running of RCO has been done on the CRAY-T3E at the Swedish National Supercomputer Centre (NSC) in Linköping. Data have been used from the Ice Data Bank for Baltic Sea climate studies, IDA (Haapala et al., 1996). Special thanks are given to Nils Kajrup for providing oceanographic profile data from the Swedish Ocean Archive SHARK (Svenskt HavsARKiv, SMHI), to Barry Broman for providing sea level data and to Jouni Räisänen for providing Figure 13b and the digitized time evolution data of the ice cover in the Baltic Sea from the ice atlas published by SMHI and FIMR (1982). Very helpful comments on an earlier draft have been made by Bertil Håkansson and also by Ralf Döscher.

References

Axell, L.B. (1998): On the variability of Baltic Sea deepwater mixing. *J. Geophys. Res.*, **103** (C10), 21667 - 21682

Beckmann, A. and R. Döscher (1997): A method for improved representation of dense water spreading over topography in geopotential-coordinate models. *J. Phys. Oceanogr.*, **27**, 581-591

Bergström, S. and B. Carlsson (1994): River runoff to the Baltic Sea: 1950-1990. *Ambio*, **23**, 280-287

Blanke, B. and P. Delecluse (1993): Variability of the Tropical Atlantic Ocean simulated by a general circulation model with two different mixed layer physics. *J. Phys. Oceanogr.*, **23**, 1363-1388

Döscher, R. and A. Beckmann (1999): Effects of a bottom boundary layer parameterization in a coarse resolution model of the North-Atlantic Ocean. *J. Atmosph. and Oceanic Tech.* , (accepted)

Ekman, M. and J. Mäkinen (1996): Mean sea surface topography in the Baltic sea and its transition area to the North Sea: A geodetic solution and comparison with oceanographic models. *J. Geophys. Res.*, **101** (C5), 11993-11999

Haapala, J. (1999): On the modelling of the ice thickness redistribution. *Journal of Glaciology*, (submitted)

Haapala, J., P. Alenius, J. Dubra, S.V. Klyachkin, T. Kouts, M. Leppäranta, A. Omstedt, L. Pakstys, N. Schmelzer, C. Schrum, A. Seinä, K. Strübing, M. Sztobryn, and E. Zaharchenko (1996): IDA - Ice data bank for Baltic Sea climate studies. *Report series in Geophysics, University of Helsinki*, **35**, 45 pp

Haapala, J. and M. Leppäranta (1996): Simulating the Baltic Sea ice season with a coupled ice-ocean model. *Tellus*, **48A**, 622 - 643

Harvey, L.D.D. (1988): Development of a sea ice model for use in zonally averaged energy balance climate models. *Journal of climate*, **1**, 1221 - 1238.

Hibler, W. D. (1979): A dynamic thermodynamic sea ice model. *J. Phys. Oceanogr.*, **9**, 817-846.

Hunke, E. C. and J. K. Dukowicz (1997): An elastic-viscous-plastic model for sea ice dynamics. *J. Phys. Oceanogr.*, **27**, 1849-1867.

Hunke, E. C. and Y. Zhang (1999): Recent Arctic Sea Ice Change Simulated with a Coupled Ice-Ocean Model. *J. of Geophys. Res.*, (submitted)

Jakobsen, F. (1997): Hydrographic investigation of the Northern Kattegat front. *Contin. Shelf Res.*, **17**, 533-554

Janssen, F., C. Schrum and J.O. Backhaus (1999): A climatological data set of temperature and salinity for the North Sea and the Baltic Sea. *Dt. Hydrogr. Z.*, (accepted)

Kielmann, J. (1981): Grundlagen und Anwendung eines numerischen Modells der geschichteten Ostsee. *Ber. Inst. f. Meeresk., Kiel*, **87 a/b**, 158/116 pp

Ledwell, J. R., A. J. Watson and C. S. Law (1993): Evidence for slow mixing across the pycnocline from an open-ocean tracer-release experiment. *Nature*, **364**, 701 - 703

Lehmann, A. (1995): A three-dimensional baroclinic eddy-resolving model of the Baltic Sea. *Tellus*, **47A**, 1013-1031

Matthäus, W. and H. Franck (1992): Characteristics of major Baltic inflows — a statistical analysis. *Contin. Shelf Res.*, **12**, 1375-1400

Matthäus, W., H.-U. Lass and R. Tiesel (1993): The major Baltic inflow in January 1993. ICES Statutory Meeting. ICES C.M. 1993/C:51

Mälkki, P. and R. Tamsalu (1985): Physical features of the Baltic Sea. *Finnish Mar. Res.*, **252**, 110 pp

Meier, H.E.M. and W. Krauß (1994): Data assimilation into a numerical model of the Baltic Sea using the adjoint method. In: *Proceedings of the* 19^{th} *Conference of the Baltic Oceanographers*, Sopot, Poland, 447-458

Meier, H.E.M. (1996): A regional model of the western Baltic Sea with open boundary conditions and data assimilation (in German). *Ber. Inst. f. Meereskunde, Kiel, Germany*, **284**, 117 pp

Meier, H.E.M. (1998): SWECLIM workshop on modelling sea ice coupled to a 3D Baltic Sea model held at SMHI, November 19 and 20, 1998. *SWECLIM Newsletter*, **3**, 31 - 34

Meier, H.E.M. (1999): Choices for parameterization of turbulence in the Baltic Sea. In: *Proceedings of the BALTEX workshop on "Parameterization of surface fluxes, atmospheric planetary boundary layer and ocean mixed layer turbulence for BRIDGE - What can we learn from field experiments"*, Abisko, Lapland, Sweden, June 20 -21, 1999, *International BALTEX Secretariat publication series*, (in press)

Meier, H.E.M., R. Döscher, A.C. Coward, J. Nycander and K. Döös (1999): RCO - Rossby Centre regional Ocean climate model: model description (version 1.0) and first results from the hindcast period 1992/93. *Reports Oceanography, SMHI*, **26**, 102 pp

Omstedt, A. (1990): Modelling the Baltic Sea as thirteen sub-basins with vertical resolution. *Tellus*, **42A**, 286-301

Omstedt, A. and L. Nyberg (1996): Response of Baltic Sea ice to seasonal, interannual forcing and climate change. *Tellus*, **48 A**, 644 - 662

Omstedt, A., L. Meuller and L. Nyberg (1997): Interannual, seasonal and regional variations of precipitation and evaporation over the Baltic Sea. *Ambio*, **26**, 484 - 492

Omstedt, A. and L.B. Axell (1998): Modelling the seasonal, interannual and long-term variations of salinity and temperature in the Baltic proper. *Tellus*, **50 A**, 637 - 652

Omstedt, A. and D. Chen (1999): Influence of atmospheric circulation on interannual variations of maximum ice extent in the Baltic Sea. (submitted)

Omstedt, A. and A. Rutgerson (1999): Closing the water and heat cylces of the Baltic Sea. *Contribution to Atmospheric Physics*, (in press)

Oschlies, A. and V. Garçon (1999): An eddy–permitting coupled physical–biological model of the North Atlantic. Part I: Sensitivity to advection numerics and mixed layer physics. *Global Biogeochem. Cycles*, **13**, 135 - 160

Rummukainen, M., J. Räisänen, A. Ullerstig, B. Bringfelt, U. Hansson, P. Graham and U. Willén (1998): RCA – Rossby Centre regional Atmospheric climate model: model description and results from the first multi-year simulation. *Reports Meteorology and Climatology, SMHI*, **83**, 76 pp

Seinä, A. and J. Peltola (1991): Duration of the ice season and statistics of fast ice thickness along the Finnish coast 1961-1990. *Finnish Marine Research*, **258**

Seinä, A., H. Grönvall, S. Kalliosaari, and J. Vainio (1996): Ice season 1991-1995 along the Finnish coast. *Meri, Report Series of the Finnish Institute of Marine Research*, **27**, 3-76

Semtner, A.J. (1976): A model for the thermodynamic growth of sea ice in numerical investigations of climate. *J. Phys. Oceanogr.*, **6**, 379 - 389

Simonsen, K. and P.M. Haugan (1996): Heat budgets of the Arctic Mediterranean and sea surface heat flux parameterizations for the Nordic Seas. *J. Geophys. Res.*, **101** (C3), 6553-6576

SMHI and FIMR (1982): Climatological Ice Atlas for the Baltic Sea, Kattegat, Skagerrak and Lake Vänern (1963-1979). Norrköping, Sweden, 220 pp

Stigebrandt, A. (1983): A model for the exchange of water and salt between the Baltic and the Skagerrak. *J. Phys. Oceanogr.*, **13**, 411-427

Stigebrandt, A. (1987): A model of the vertical circulation of the Baltic deep water. *J. Phys. Oceanogr.*, **17**, 1772-1785

Stigebrandt, A. (1995): The large-scale vertical circulation of the Baltic Sea. In: *First Study Conference on BALTEX*, Visby, Sweden, August 28 - September 1, 1995, edited by A. Omstedt, *International BALTEX Secretariat publication series*, **3**, 28 - 47

SWECLIM (1998): Regional climate simulations for the Nordic region – First results from SWECLIM. SMHI, November, 1998, 22 pp

Webb, D.J., B.A. de Cuevas and C.S. Richmond (1998): Improved advection schemes for ocean models. *J. Atmos. Oceanic Technol.*, **15**, 1171-1187

Welander, P. (1974): Two-layer exchange in an estuary basin, with special reference to the Baltic Sea. *J. Phys. Oceanogr.*, **4**, 542-556

Zhang, Z. and M. Leppäranta (1995): Modeling the influence of ice on sea level variations on the Baltic Sea. *Geophysica*, **31** (2), 31 - 45

List of Figures

SMHIs publications

SMHI publishes six report series. Three of these, the R-series, are intended for international readers and are in most cases written in English. For the others the Swedish language is used.

Names of the Series	**Published since**
RMK (Report Meteorology och Climatology)	1974
RH (Report Hydrology)	1990
RO (Report Oceanography)	1986
METEOROLOGI	1985
HYDROLOGI	1985
OCEANOGRAFI	1985

Earlier issues published in RO

1 Lars Gidhagen, Lennart Funkquist and Ray Murthy (1986)
Calculations of horizontal exchange coefficients using Eulerian time series current meter data from the Baltic Sea.

2 Thomas Thompson (1986)
Ymer-80, satellites, arctic sea ice and weather.

3 Stig Carlberg et al (1986)
Program för miljökvalitetsövervakning - PMK.

4 Jan-Erik Lundqvist och Anders Omstedt (1987)
Isförhållandena i Sveriges södra och västra farvatten.

5 Stig Carlberg, Sven Engström, Stig Fonselius, Håkan Palmén, Eva-Gun Thelén, Lotta Fyrberg och Bengt Yhlen (1987)
Program för miljökvalitetsövervakning - PMK. Utsjöprogram under 1986.

6 Jorge C. Valderama (1987)
Results of a five year survey of the distribution of UREA in the Baltic sea.

7 Stig Carlberg, Sven Engström, Stig Fonselius, Håkan Palmén, Eva-Gun Thelén, Lotta Fyrberg, Bengt Yhlen och Danuta Zagradkin (1988).
Program för miljökvalitetsövervakning - PMK. Utsjöprogram under 1987.

8 Bertil Håkansson (1988)
Ice reconnaissance and forecasts in Storfjorden, Svalbard.

9 Stig Carlberg, Sven Engström, Stig Fonselius, Håkan Palmén, Eva-Gun Thelén, Lotta Fyrberg, Bengt Yhlen, Danuta Zagradkin, Bo Juhlin och Jan Szaron (1989)
Program för miljökvalitetsövervakning - PMK. Utsjöprogram under 1988.

10 L. Fransson, B. Håkansson, A. Omstedt och L. Stehn (1989)
Sea ice properties studied from the icebreaker Tor during BEPERS-88.

11 Stig Carlberg, Sven Engström, Stig Fonselius, Håkan Palmén, Lotta Fyrberg, Bengt Yhlen, Bo Juhlin och Jan Szaron (1990)
Program för miljökvalitetsövervakning - PMK. Utsjöprogram under 1989.

12 Anders Omstedt (1990)
Real-time modelling and forecasting of temperatures in the Baltic Sea.

13 Lars Andersson, Stig Carlberg, Elisabet Fogelqvist, Stig Fonselius, Håkan Palmén, Eva-Gun Thelén, Lotta Fyrberg, Bengt Yhlen och Danuta Zagradkin (1991)
Program för miljökvalitetsövervakning - PMK. Utsjöprogram under 1990.

14 Lars Andersson, Stig Carlberg, Lars Edler, Elisabet Fogelqvist, Stig Fonselius, Lotta Fyrberg, Marie Larsson, Håkan Palmén, Björn Sjöberg, Danuta Zagradkin, och Bengt Yhlen (1992)
Haven runt Sverige 1991. Rapport från SMHI, Oceanografiska Laboratoriet, inklusive PMK - utsjöprogrammet. (The conditions of the seas around Sweden. Report from the activities in 1991, including PMK - The National Swedish Programme for Monitoring of Environmental Quality Open Sea Programme.)

15 Ray Murthy, Bertil Håkansson and Pekka Alenius (ed.) (1993)
The Gulf of Bothnia Year-1991 - Physical transport experiments.

16 Lars Andersson, Lars Edler and Björn Sjöberg (1993)
The conditions of the seas around Sweden. Report from activities in 1992.

17 Anders Omstedt, Leif Nyberg and Matti Leppäranta (1994)
A coupled ice-ocean model supporting winter navigation in the Baltic Sea.
Part 1. Ice dynamics and water levels.

18 Lennart Funkquist (1993)
An operational Baltic Sea circulation model. Part 1. Barotropic version.

19 Eleonor Marmefelt (1994)
Currents in the Gulf of Bothnia. During the Field Year of 1991.

20 Lars Andersson, Björn Sjöberg and Mikaell Krysell (1994)
The conditions of the seas around Sweden. Report from the activities in 1993.

21 Anders Omstedt and Leif Nyberg (1995)
A coupled ice-ocean model supporting winter navigation in the Baltic Sea.
Part 2. Thermodynamics and meteorological coupling.

22 Lennart Funkquist and Eckhard Kleine (1995)
Application of the BSH model to Kattegat and Skagerrak.

23 Tarmo Köuts and Bertil Håkansson (1995)
Observations of water exchange, currents, sea levels and nutrients in the Gulf of Riga.

24 Urban Svensson (1998)
PROBE An Instruction Manual.

25 Maria Lundin (1999)
Time Series Analysis of SAR Sea Ice Backscatter Variability and its Dependence on Weather Conditions.

26 Markus Meier[1], Ralf Döscher[1], Andrew, C. Coward[2], Jonas Nycander[3] and Kristofer Döös[3] (1999). RCO – Rossby Centre regional Ocean climate model: model description (version 1.0) and first results from the hindcast period 1992/93.
[1] Rossby Centre, SMHI [2] James Rennell Division, Southampton Oceanography Centre, [3] Department of Meteorology, Stockholm University

SMHI

Swedish Meteorological and Hydrological Institute
SE 601 76 Norrköping, Sweden.
Tel +46 11-495 80 00 · Fax +46 11-495 80 01

ISSN 0283-1112